Tools for the Analysis of Non-Normal Fluid Systems

Peter Schmid

Laboratoire d'Hydrodynamique (LadHyX)

CNRS-Ecole Polytechnique, Palaiseau

Int'l Summer School & Workshop on Non-Normal and Nonlinear Effects In Aero- and Thermoacoustics
Technische Universität München
May 17-20, 2010

Hydrodynamic stability

Stability theory is concerned with the *behavior* of a fluid system with respect to a predefined base state.

Stability theory is a central discipline of fluid dynamics.

Stability has to be defined carefully.

Stability is parameter-dependent.

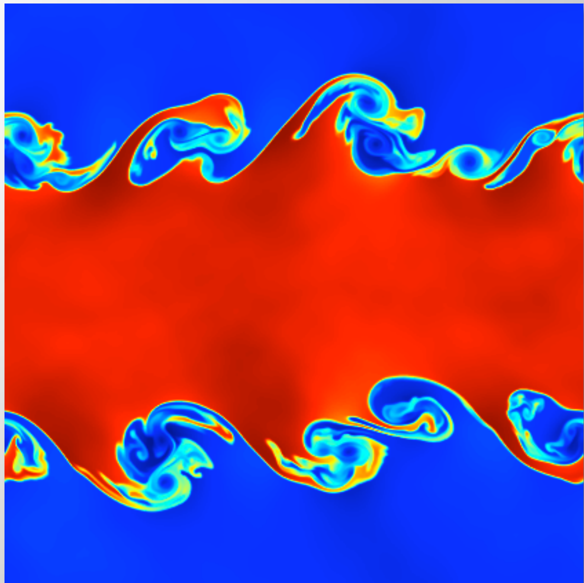

Two concepts of stability

Linear stability: we are interested in the ***minimum*** critical parameter above which a specific initial condition of ***infinitesimal*** amplitude grows ***exponentially***

Energy stability: we are interested in the ***maximum*** critical parameter below which a general initial condition of ***finite*** amplitude decays ***monotonically***

Two examples

Example 1: **Rayleigh-Bénard convection** (onset of convective instabilities can be described as an instability of the conductive state)

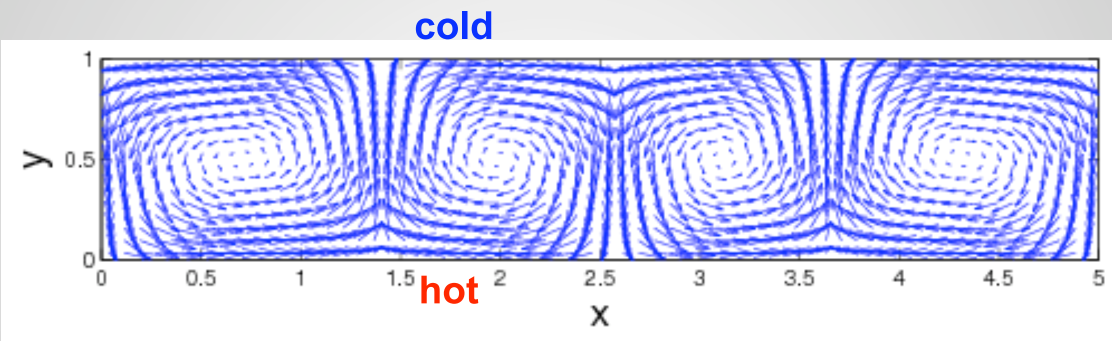

Rayleigh number (a non-dimensionalized temperature gradient) is the governing parameter

Linear stability theory: above a critical Rayleigh number of **1708** the conductive state becomes unstable to infinitesimal perturbations

Energy stability theory: below a critical Rayleigh number of **1708** finite-amplitude perturbations superimposed on the conductive state decay monotonically in energy

Experiments: show the onset of convective instabilities at a critical Rayleigh number of about **1710**

Two examples

Example 2: **Plane Poiseuille flow** (breakdown of the parabolic mean velocity profile)

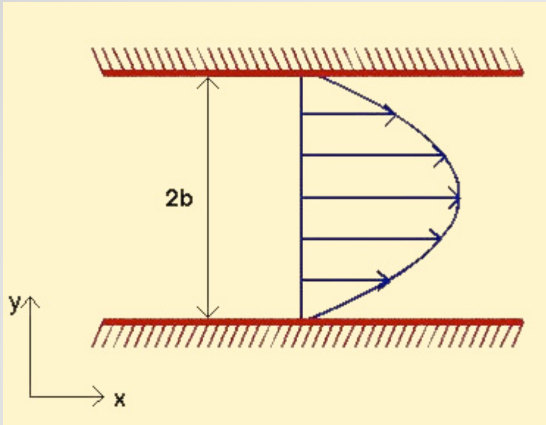

Reynolds number (a non-dimensionalized velocity) is the governing parameter

Linear stability theory: above a critical Reynolds number of **5772** the parabolic velocity profile becomes unstable to infinitesimal perturbations

Energy stability theory: below a critical Reynolds number of **49.6** finite-amplitude perturbations superimposed on the parabolic velocity profile decay monotonically in energy

Experiments: show the breakdown of the parabolic velocity profile at a critical Reynolds number of about **1000**

Two examples

Linear stability theory, energy stability theory and experiments are in excellent agreement for Rayleigh-Bénard convection

Linear stability theory, energy stability theory and experiments show significant discrepancies for plane Poiseuille flow

Questions:

Can we explain the success and failure of stability theory for the above two examples?

Is there a better way of investigating the stability of plane Poiseuille flow (and many other wall-bounded shear flows)?

A paradox

Fact:

The nonlinear terms in the Navier-Stokes equations conserve energy.

Fact:

During transition to turbulence we observe a substantial increase in kinetic perturbation energy, even for Reynolds numbers below the critical one.

Conclusion:

The increase in energy for subcritical Reynolds numbers has to be accomplished by a linear process, without relying on an exponential instability; i.e. we need *a linear instability without an unstable eigenvalue*.

Starting point are the $\boxed{\text{Navier-Stokes equations}}$ (assuming incompressible flow)

decomposition of the flow field into mean and perturbation

$$\mathbf{u} = \mathbf{U} + \varepsilon \mathbf{u}'$$

further simplifying assumptions: uni-directional mean flow dependent on one spatial coordinate, e.g.,

$$\mathbf{U} = U(y)\hat{\mathbf{x}}$$

further simplifying assumptions: wave-like perturbation in the homogeneous directions

$$\mathbf{u} = \hat{\mathbf{u}}(y) \exp(i\alpha x + i\beta z)$$

it is convenient to eliminate the pressure (and the continuity equation) by choosing the normal velocity and normal vorticity as the dependent variables

$$\frac{\partial}{\partial t}\begin{pmatrix}\hat{v}\\ \hat{\eta}\end{pmatrix} = \begin{pmatrix}\mathcal{L}_{OS} & 0\\ \mathcal{L}_{C} & \mathcal{L}_{SQ}\end{pmatrix}\begin{pmatrix}\hat{v}\\ \hat{\eta}\end{pmatrix}$$

$\mathcal{L}_{OS}$ = Orr-Sommerfeld operator

$\mathcal{L}_{SQ}$ = Squire operator

$\mathcal{L}_{C}$ = coupling operator

Final step: discretization in the inhomogeneous direction (y) using spectral, compact- or finite-difference methods

$$\frac{d}{dt}\begin{pmatrix} v \\ \eta \end{pmatrix} = \underbrace{\begin{pmatrix} L_{OS} & 0 \\ L_C & L_{SQ} \end{pmatrix}}_{L} \underbrace{\begin{pmatrix} v \\ \eta \end{pmatrix}}_{q}$$

$$\boxed{\frac{d}{dt}q = Lq}$$

Formally, this equation has a solution in form of the matrix exponential of L.

$$\boxed{\frac{d}{dt}q = Lq}$$

$$\boxed{q = \exp(tL)q_0} \qquad q_0 = q(t=0)$$

The matrix exponential of L is the stability operator after the linearization step.

$$q = \exp(tL)q_0$$

We can redefine the concept of stability based on the matrix exponential by considering the growth of perturbation energy over time.

$$G(t) = \max_{q_0} \frac{\|q\|^2}{\|q_0\|^2} = \|\exp(tL)\|^2$$

G(t) represents the amplification of perturbation energy maximized over all initial conditions.

In general, the matrix exponential is difficult to compute. In its place, eigenvalues of L have been used as proxies.

$$L = S\Lambda S^{-1}$$

eigenvalue decomposition

$$\|\exp(tL)\|^2 = \|\exp(tS\Lambda S^{-1})\|^2 = \|S\,\boxed{\exp(t\Lambda)}\,S^{-1}\|^2$$

traditional stability analysis

In traditional stability analysis, the behavior of G(t) is deduced from the eigenvalues of L.

Do the eigenvalues of L capture the behavior of G(t) ?

We can answer this question by computing upper and lower bounds (estimates) on G(t).

The energy cannot decay at a faster rate than the one given by the least stable eigenvalue λ_{max}

lower bound

$$\mathrm{e}^{2\mathrm{t}\lambda_{\mathrm{max}}} \leq \|\exp(\mathrm{tL})\|^2$$

For the upper bound we use the eigenvalue decomposition of L.

upper bound

$$\begin{aligned} \|\exp(tL)\|^2 &= \|S\exp(t\Lambda)S^{-1}\|^2 \\ &\leq \|S\|^2\|S^{-1}\|^2\mathrm{e}^{2\mathrm{t}\lambda_{\mathrm{max}}} \end{aligned}$$

We can answer this question by computing upper and lower bounds (estimates) on G(t).

$$e^{2t\lambda_{\max}} \leq \|\exp(tL)\|^2 \leq \boxed{\|S\|^2\|S^{-1}\|^2} e^{2t\lambda_{\max}}$$

1 or $\gg 1$

Two cases can be distinguished:

$\kappa(S) = \|S\|^2\|S^{-1}\|^2 = 1$ upper and lower bound coincide: the energy amplification is governed by the least stable eigenvalue

$\kappa(S) = \|S\|^2\|S^{-1}\|^2 \gg 1$ upper and lower bound can differ significantly: the energy amplification is governed by the least stable eigenvalue ***only for large times***

This suggests distinguishing two different classes of stability problems.

$$\kappa(S) = \|S\|^2\|S^{-1}\|^2 = 1$$

<u>normal</u> stability problems

- orthogonal eigenvectors
- eigenvalye analysis captures the dynamics

$$\kappa(S) = \|S\|^2\|S^{-1}\|^2 \gg 1$$

<u>nonnormal</u> stability problems

- non-orthogonal eigenvectors
- eigenvalye analysis captures the asymptotic dynamics, but not the short-time behavior

The nonnormality of the system can give rise to transient energy amplification.

Even though we experience exponential decay for large times, the non-orthogonal superposition of eigenvectors can lead to short-time growth of energy.

Geometric interpretation:

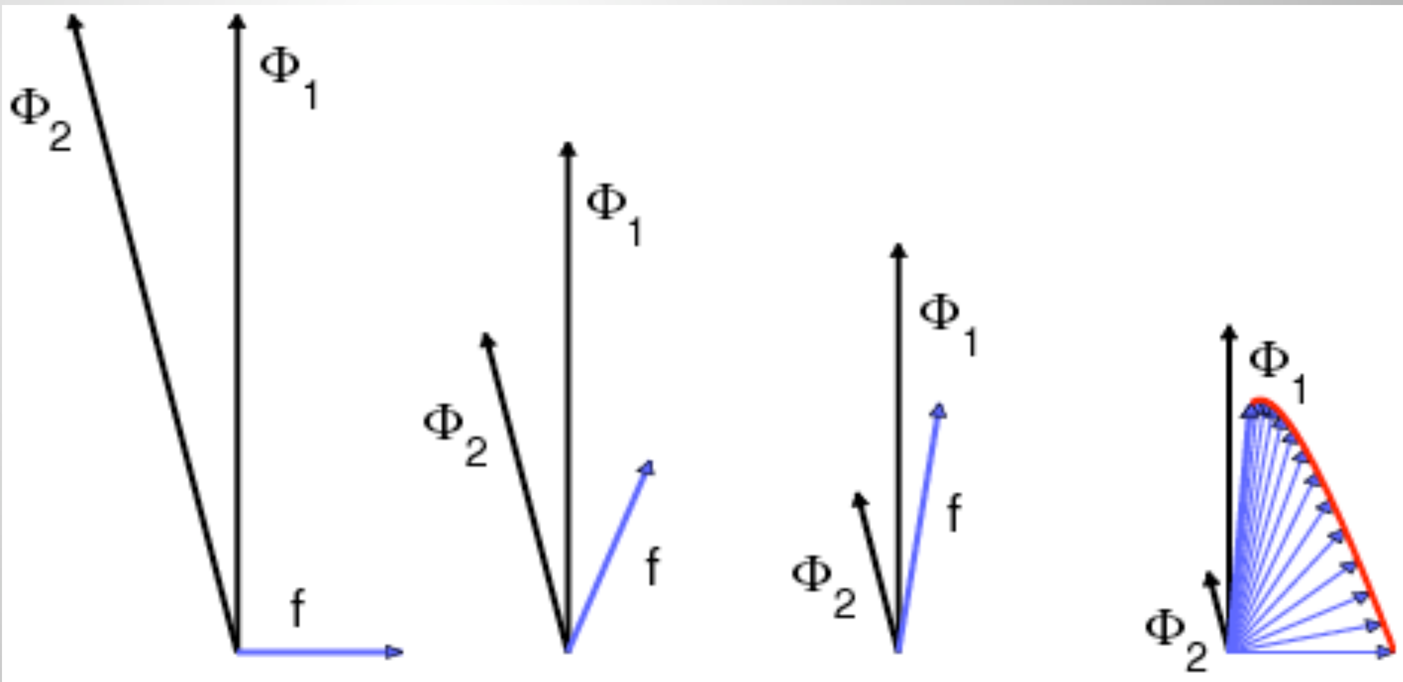

Is there a better way of describing the short-time dynamics of nonnormal stability problems ?

$$\kappa(S) = \|S\|^2 \|S^{-1}\|^2 \gg 1$$

We start with a Taylor expansion of the matrix exponential about t=0.

$$\begin{aligned} E(t) &= \langle q, q \rangle = \|q\|^2 \\ &= \langle \exp(tL) q_0, \exp(tL) q_0 \rangle \\ &\approx \langle (I + tL) q_0, (I + tL) q_0 \rangle \\ &\approx \langle q_0, q_0 \rangle + t \; \langle q_0, (L + L^H) q_0 \rangle \end{aligned}$$

$$E(t) \approx \langle q_0, q_0 \rangle + t \ \langle q_0, (L + L^H) q_0 \rangle$$

The initial energy growth rate is given by

$$\frac{1}{E} \left. \frac{dE}{dt} \right|_{t=0^+} = \frac{\langle q_0, (L + L^H) q_0 \rangle}{\langle q_0, q_0 \rangle}$$

$(L + L^H)$ is Hermitian (symmetric)

$$\frac{1}{E} \left. \frac{dE}{dt} \right|_{t=0^+} = \lambda_{\max}(L + L^H)$$

numerical abscissa of L

The numerical abscissa can be generalized to the ***numerical range***.

$$\frac{d}{dt}\|q\|^2 = \left\langle \frac{d}{dt}q, q \right\rangle + \left\langle q, \frac{d}{dt}q \right\rangle$$

$$= \langle Lq, q\rangle + \langle q, Lq\rangle$$

$$= 2\mathrm{Real}\left\{\langle Lq, q\rangle\right\}$$

Definition of the numerical range:

$$\mathcal{F}(L) = \left\{ z \mid z = \frac{\langle Lq, q\rangle}{\langle q, q\rangle} \right\}$$

set of all Rayleigh quotients of L

$$\mathcal{F}(L) = \left\{ z \mid z = \frac{\langle Lq, q\rangle}{\langle q, q\rangle} \right\}$$

set of all Rayleigh quotients of L

Three important properties of the numerical range:

1. The numerical range is convex.

2. The numerical range contains the spectrum of L.

3. For normal L, the numerical range is the convex hull of the spectrum.

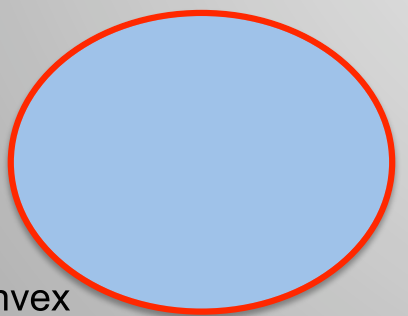

convex

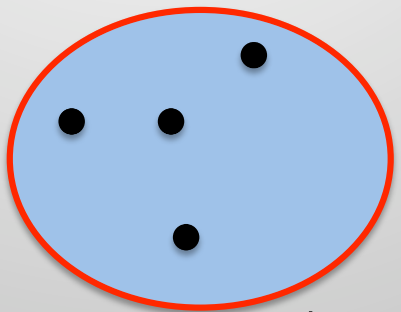

contains spectrum

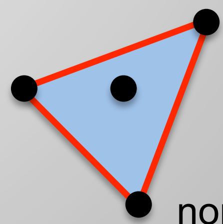

normal case

$$\mathcal{F}(L) = \left\{ z \mid z = \frac{\langle Lq, q\rangle}{\langle q, q\rangle} \right\}$$

set of all Rayleigh quotients of L

Illustration:

$$A = \begin{pmatrix} -5 & 4 & 4 \\ & -2-2i & 4 \\ & & -0.3+i \end{pmatrix}$$

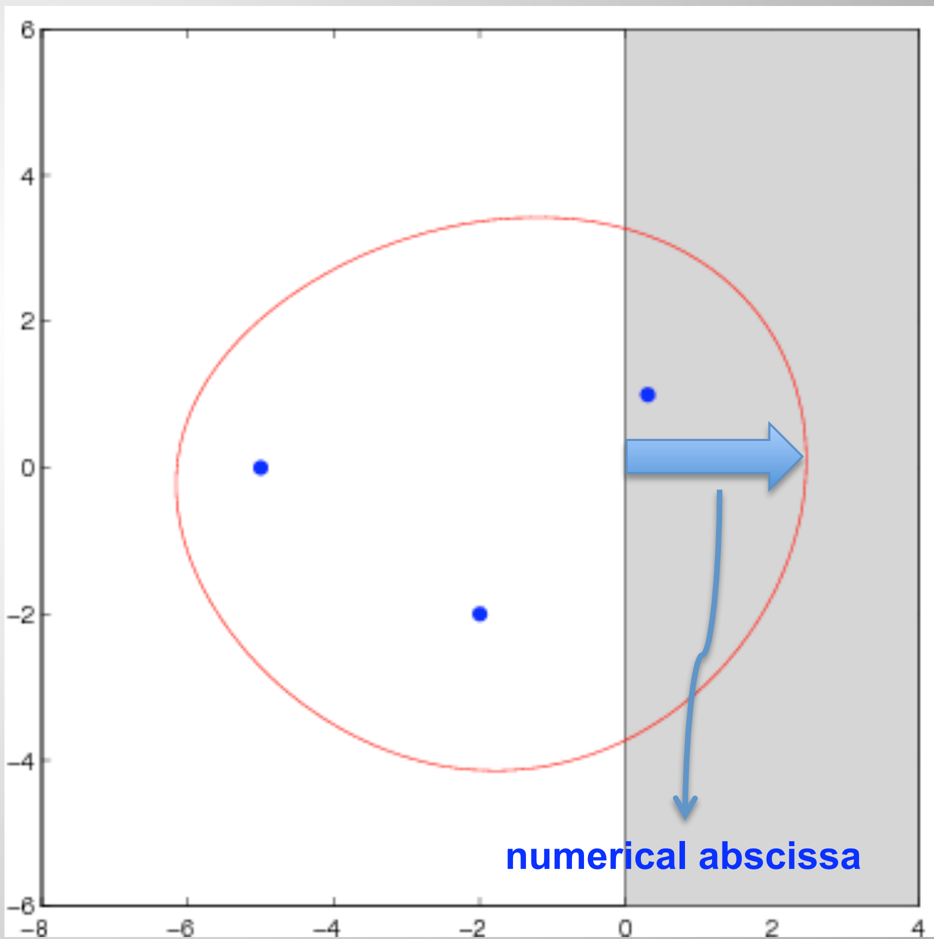

The numerical range is substantially larger than the convex hull of the spectrum.

$$\mathcal{F}(L) = \left\{ z \mid z = \frac{\langle Lq, q \rangle}{\langle q, q \rangle} \right\}$$ set of all Rayleigh quotients of L

Illustration:

$$A = \begin{pmatrix} -5 & & \\ & -2-2i & \\ & & -0.3+i \end{pmatrix}$$

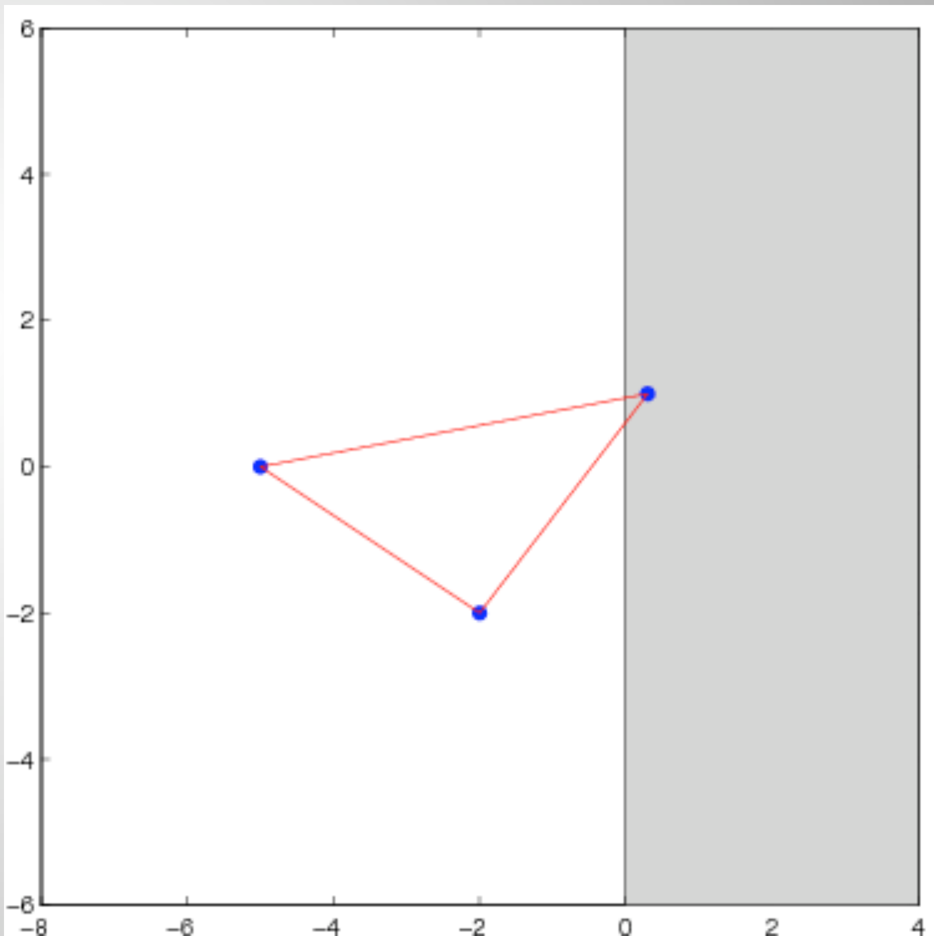

The numerical range is the convex hull of the spectrum.

For nonnormal stability problems:

The numerical abscissa (numerical range) governs the very short time behavior. The sign of the numerical abscissa determines initial energy growth or decay.

The least stable eigenvalue governs the long time behavior. The sign of the real part of $\lambda_{\max}$ determines asymptotic energy growth or decay.

revisit Rayleigh-Bénard convection and plane Poiseuille flow

Rayleigh-Bénard convection is a **normal** stability problem

The numerical range is the convex hull of the spectrum.

The numerical range and the spectrum cross into the unstable half-plane at the same Rayleigh number.

Initial energy growth and asymptotic instability occur at the same Rayleigh number.

$$Ra_{lin} = Ra_{ener} = 1708$$

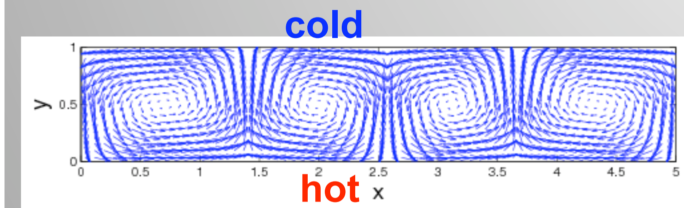

The spectrum governs the perturbation dynamics at all times.

plane Poiseuille flow is a **nonnormal** stability problem

- The numerical range is larger than the convex hull of the spectrum.
  - The numerical range crosses into the unstable half-plane « before » the spectrum crosses into the unstable half-plane.
    - Initial energy growth is possible « before » asymptotic instability occurs.
      - $$Re_{lin} = 5772 \gg Re_{ener} = 49.6$$
        - The spectrum governs the perturbation dynamics only in the asymptotic limit of $t \longrightarrow \infty$

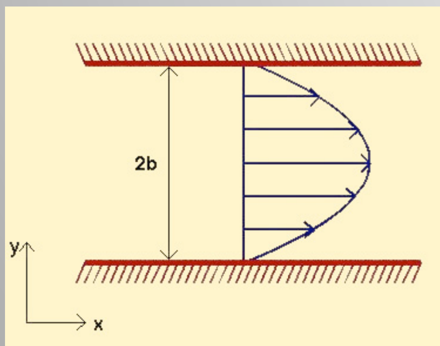

Summary

short time

$$\boxed{\left.\frac{1}{E}\frac{dE}{dt}\right|_{t=0+} = \lambda_{\max}(L + L^H)}$$

(numerical abscissa)

all time

$$\boxed{\|\exp(tL)\|^2}$$

(matrix exponential norm)

long time

$$\boxed{G(t\to\infty) = \lim_{t\to\infty}\|\exp(tL)\| = \mathrm{e}^{t\lambda_{\max}}}$$

(eigenvalues)

The energy amplification curve G(t) is the envelope over many individual growth curves.

For each point on this curve, a specific initial condition reaches its maximum energy amplification at this point (in time).

Can we recover the initial condition that results in the maximum energy amplification at a given time? $\Rightarrow$ optimal initial condition equation that governs the optimal initial condition

$$\exp(t^* L) q_0 = q(t^*)$$

q_0 input (initial condition)

$q(t^*)$ output (final condition)

Assume that the initial condition satisfies $\|q_0\| = 1$ and normalize the output such that $\|\bar{q}(t^*)\| = 1$

$$\underbrace{\exp(t^* L)}_{\text{propagator}} \; \underbrace{\bar{q}_0}_{\text{input}} = \underbrace{\|\exp(t^* L)\|}_{\text{amplification}} \; \underbrace{\bar{q}(t^*)}_{\text{output}}$$

$$\underset{\text{propagator}}{\exp(t^* L)} \; \underset{\text{input}}{\bar{q}_0} = \underset{\text{amplification}}{\| \exp(t^* L) \|} \; \underset{\text{output}}{\bar{q}(t^*)}$$

The singular-value decomposition of a matrix A is

$$A = \underbrace{U}_{\substack{\text{unitary}\\ \text{(orthogonal)}}} \underbrace{\Sigma}_{\text{diagonal}} \underbrace{V^H}_{\substack{\text{unitary}\\ \text{(orthogonal)}}}$$

$$\underbrace{\exp(t^* L)}_{\text{propagator}} \; \underbrace{\bar{q}_0}_{\text{input}} = \underbrace{\| \exp(t^* L) \|}_{\text{amplification}} \; \underbrace{\bar{q}(t^*)}_{\text{output}}$$

The singular-value decomposition of a matrix A is

$$AV = U\Sigma$$

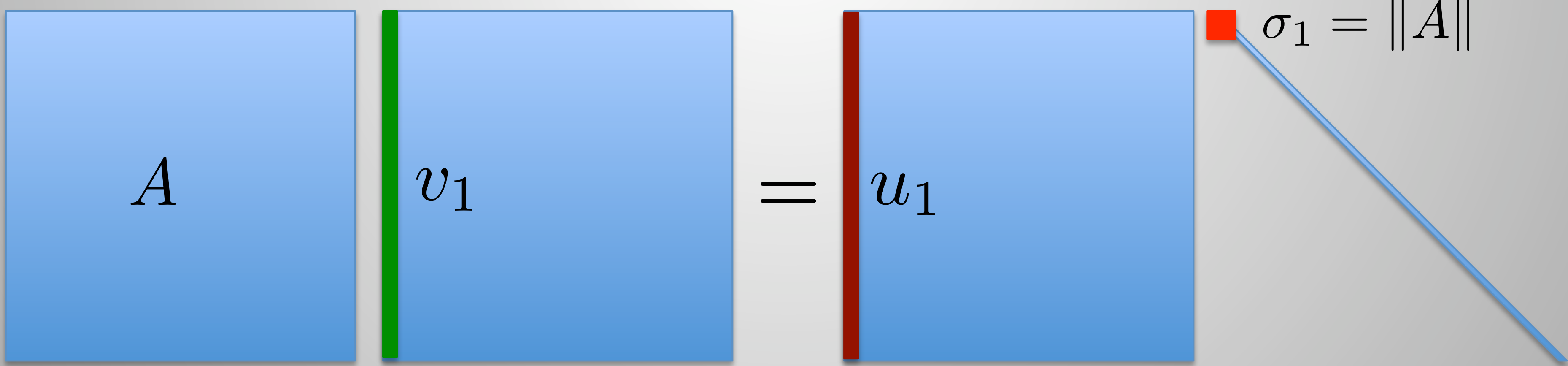

$$\exp(t^* L)\ \bar{q}_0 = \|\exp(t^* L)\|\ \bar{q}(t^*)$$

propagator input amplification output

The singular-value decomposition of our matrix exponential at t^* is

$$\text{svd}\,(\exp(t^* L)) = U \Sigma V^H$$

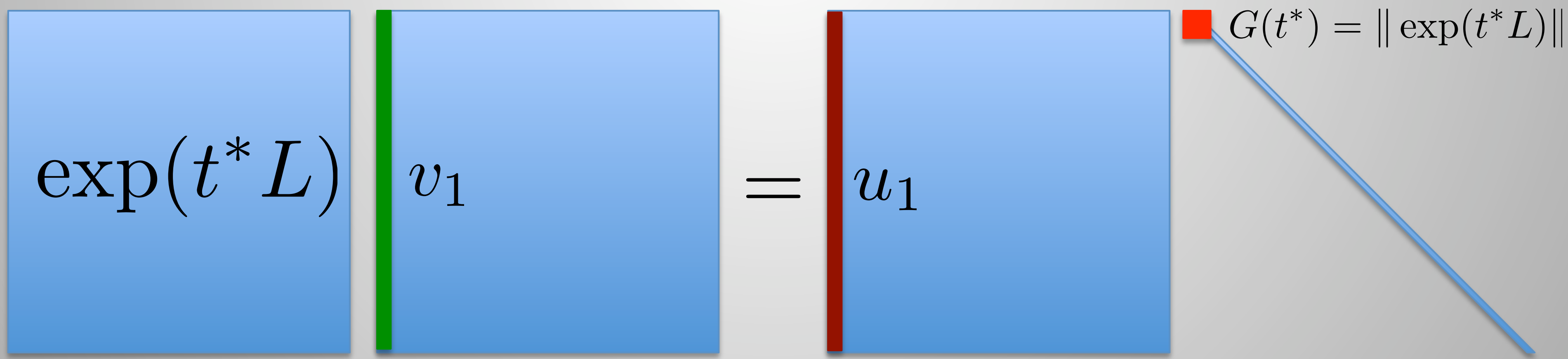

$$\exp(t^* L)\ \bar{q}_0 = \|\exp(t^* L)\|\ \bar{q}(t^*)$$

propagator input amplification output

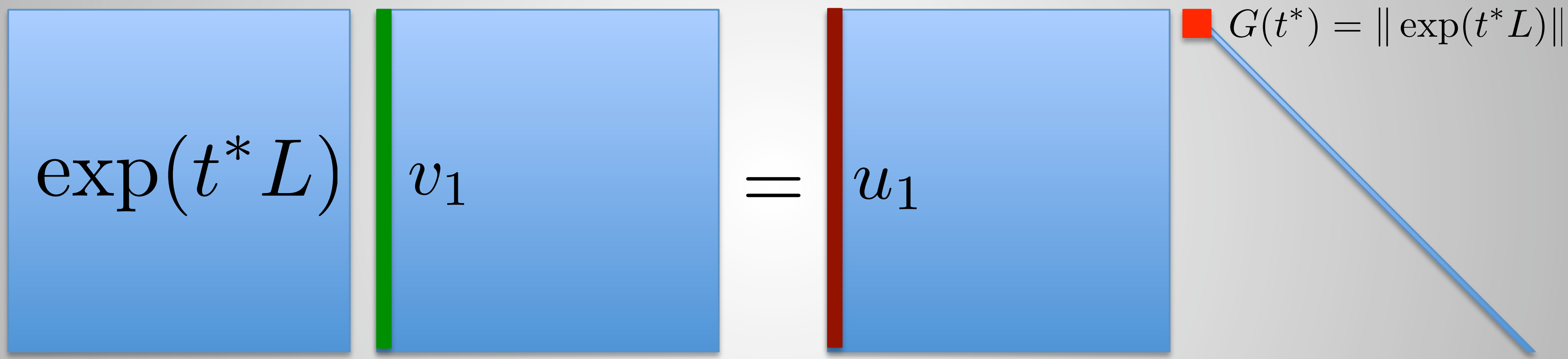

optimal initial condition is the left principal singular vector

Optimal final condition is the right principal singular vector often we are interested in the response of our fluid system to external forces (modelling free-stream turbulence, acoustic waves, wall-roughness etc.)

in this case, our governing equation can be formulated as

$$\frac{d}{dt} q = Lq + f$$

f model of external forces

the response to forcing (particular solution, i.e., zero initial condition) is

$$q_p = \int_0^t \exp((\tau - t)L) f(\tau)\ d\tau$$

(memory integral)

for the special case of harmonic forcing $f = \hat{f}\mathrm{e}^{i\omega t}$

this simplifies to

$$\hat{q}_p = (i\omega - L)^{-1}\hat{f}$$

and the optimal response (optimized over all possible forcing functions) becomes

$$R(\omega) = \max_{\hat{f}} \frac{\|\hat{q}_p\|}{\|\hat{f}\|} = \max_{\hat{f}} \frac{\|(i\omega - L)^{-1}\hat{f}\|}{\|\hat{f}\|} = \|(i\omega - L)^{-1}\|$$

(resolvent norm)

eigenvalue-based analysis recovers the classical resonance condition

$$\|(i\omega - L)^{-1}\| = \|S(i\omega - \Lambda)^{-1}S^{-1}\| \leq \kappa(S)\frac{1}{\mathrm{dist}\{i\omega, \Lambda\}}$$

for a ***normal*** system, the classical resonance condition (closeness of forcing frequency to one of the eigenfrequencies) holds

for a ***non-normal*** system, we can have a ***pseudo-resonance*** (large response to outside forcing) even though the forcing frequency is far from an eigenfrequency of the linear system to obtain the optimal forcing we proceed as before (i.e., take the svd)

$$(i\omega^* - L)^{-1}\ \bar{f} = \|(i\omega^* - L)^{-1}\|\ \bar{q}_p$$

transfer function | forcing (unit energy) | amplification | response (unit energy)

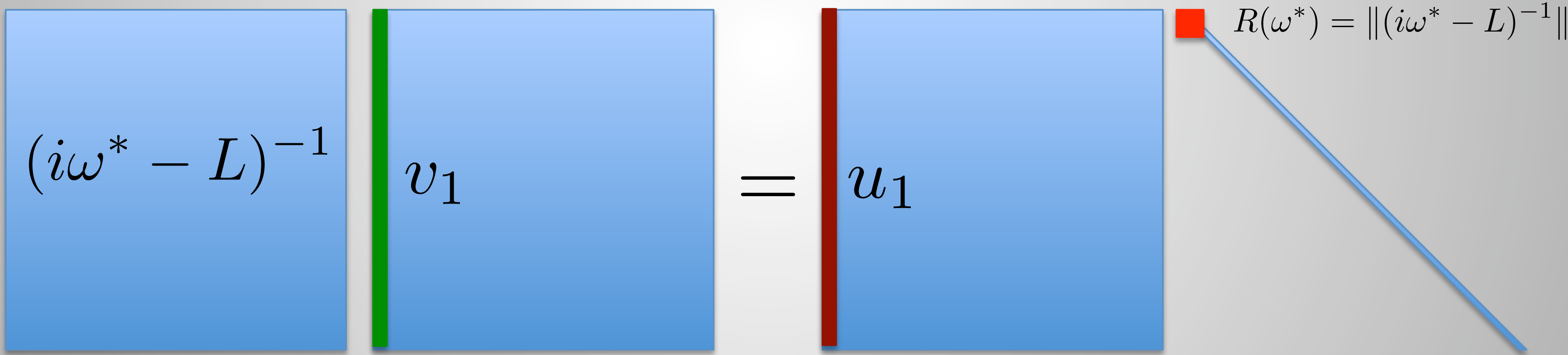

optimal harmonic forcing
is the left principal
singular vector

optimal harmonic response
is the right principal
singular vector

Example: plane Poiseuille flow

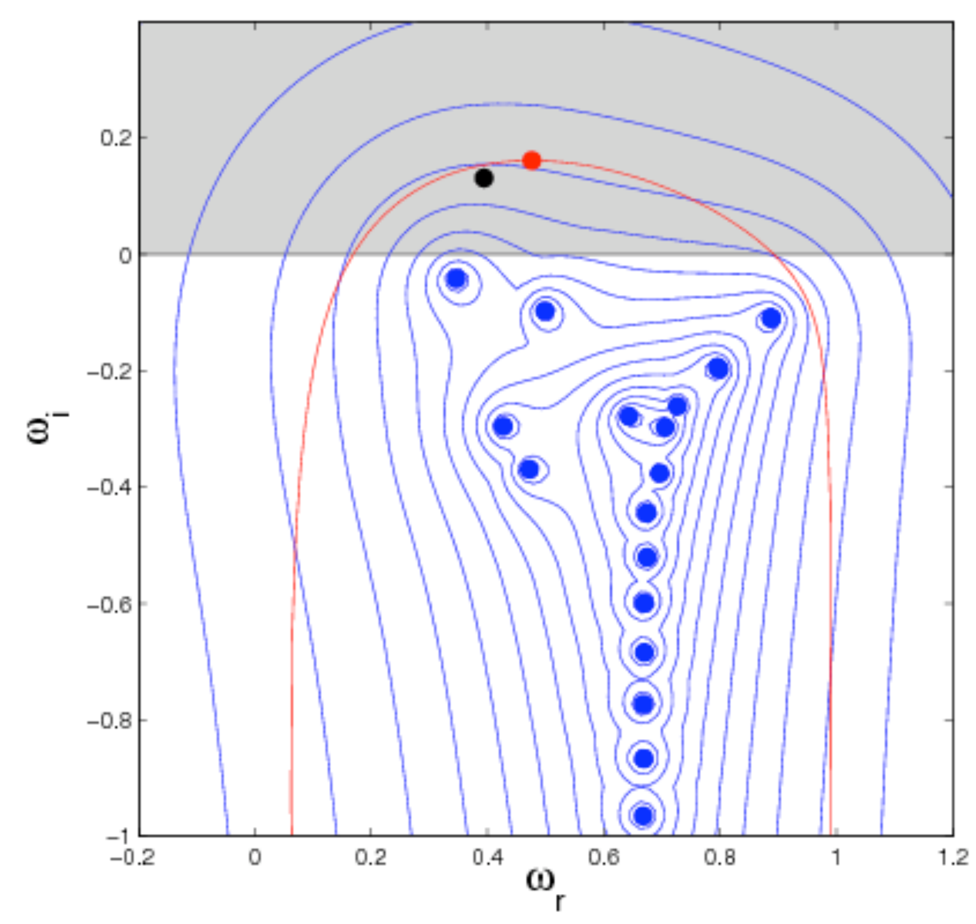

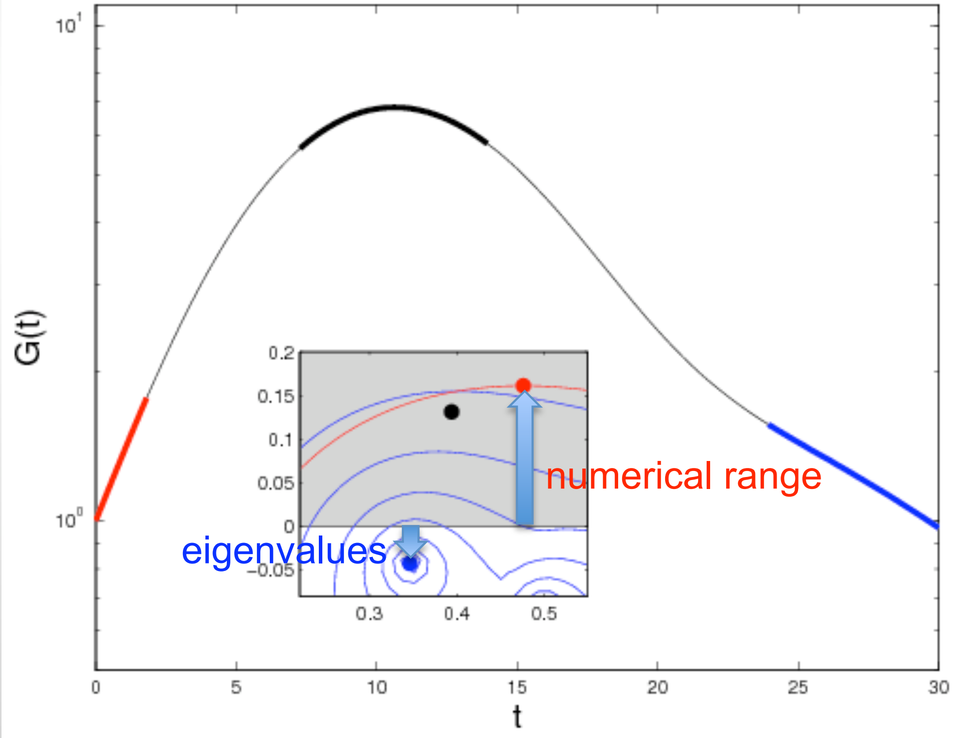

Example: plane Poiseuille flow

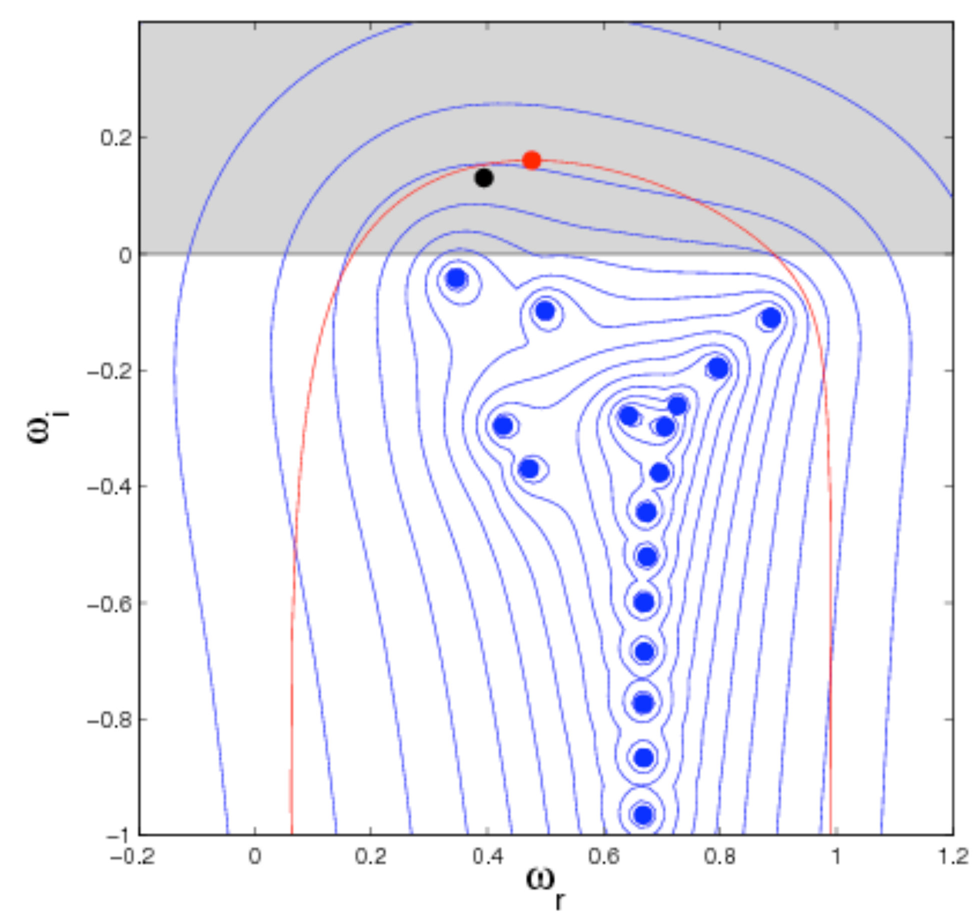

neutral curve

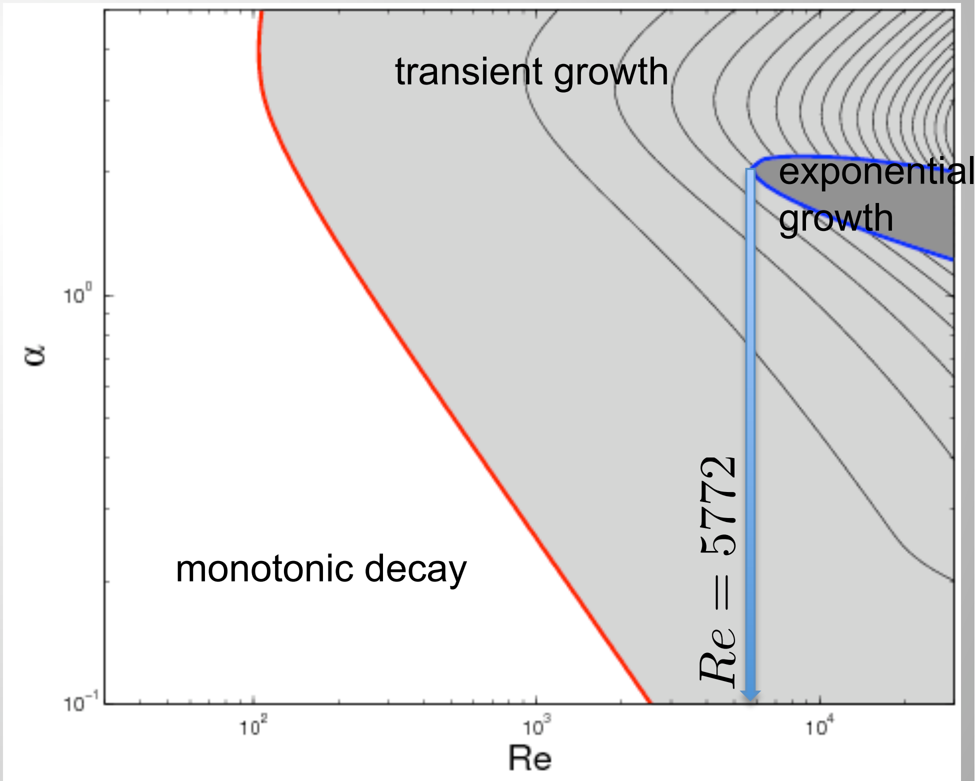

Example: plane Poiseuille flow

$\alpha = 1 \quad \beta = 1 \quad Re = 2500$

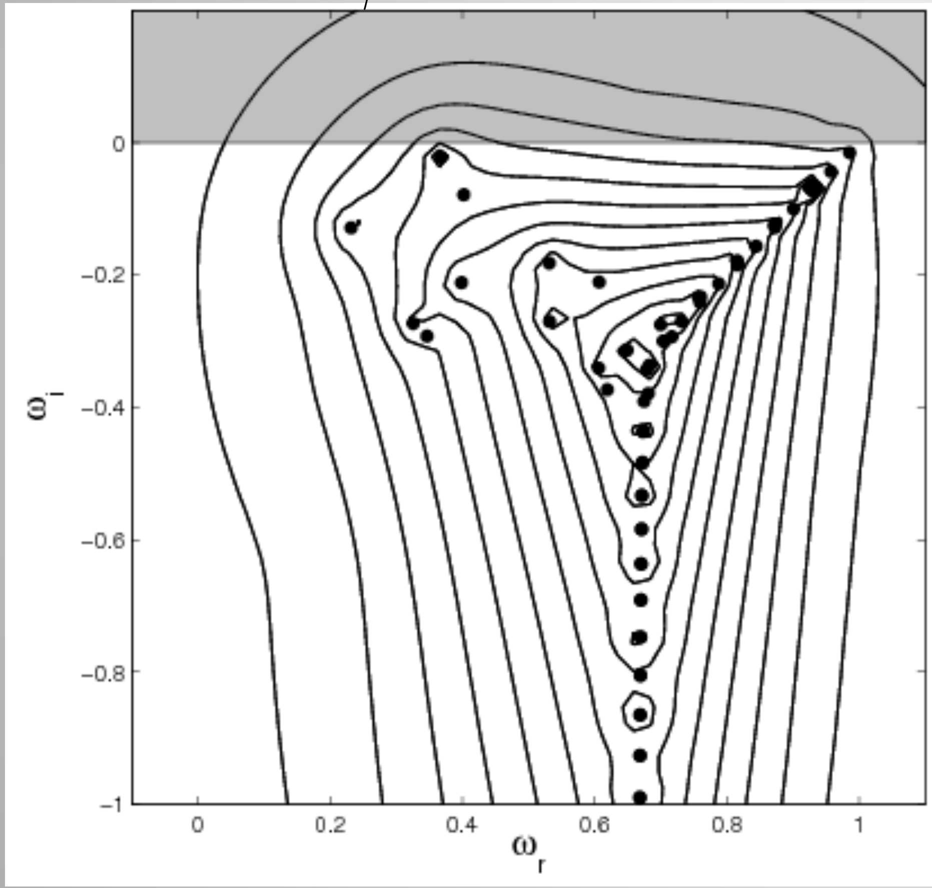

$\alpha = 0 \quad \beta = 2 \quad Re = 2500$

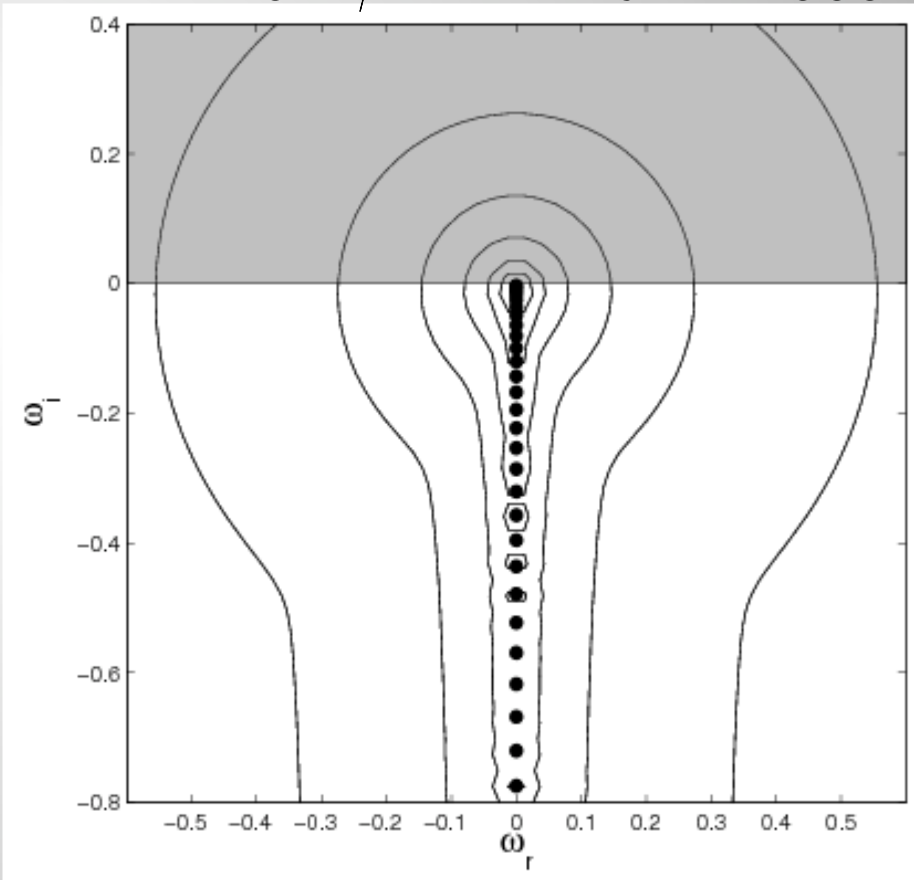

Example: plane Poiseuille flow

$$\alpha = 1 \quad \beta = 1 \quad Re = 2500$$

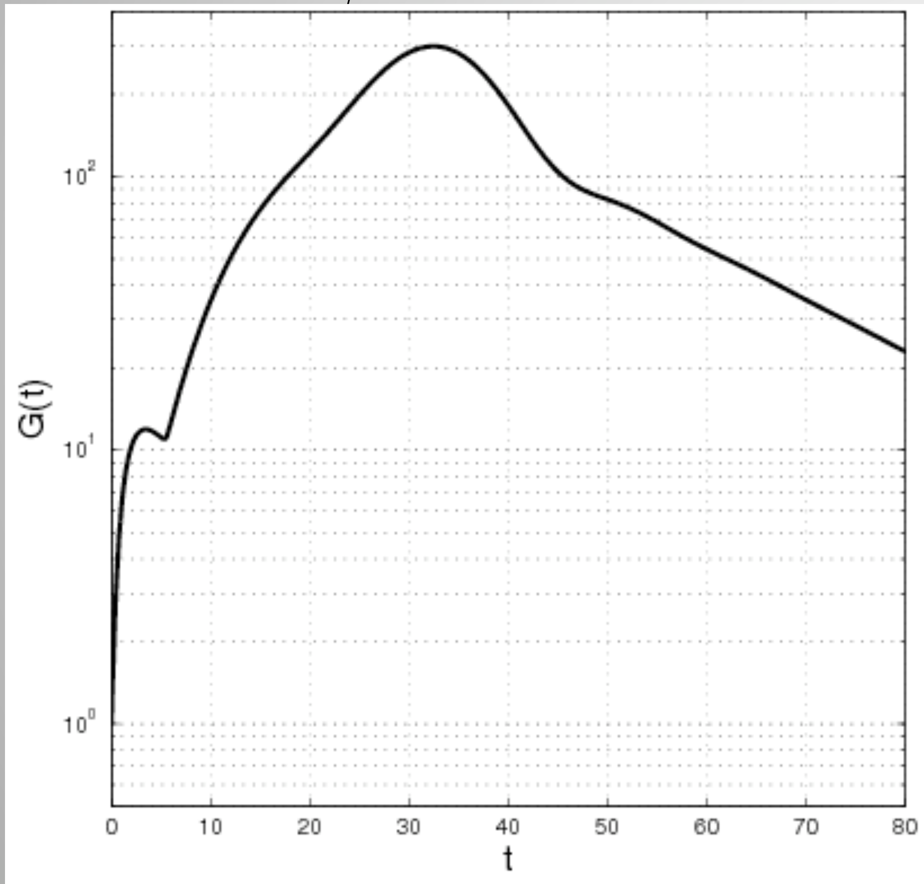

$$\alpha = 0 \quad \beta = 2 \quad Re = 2500$$

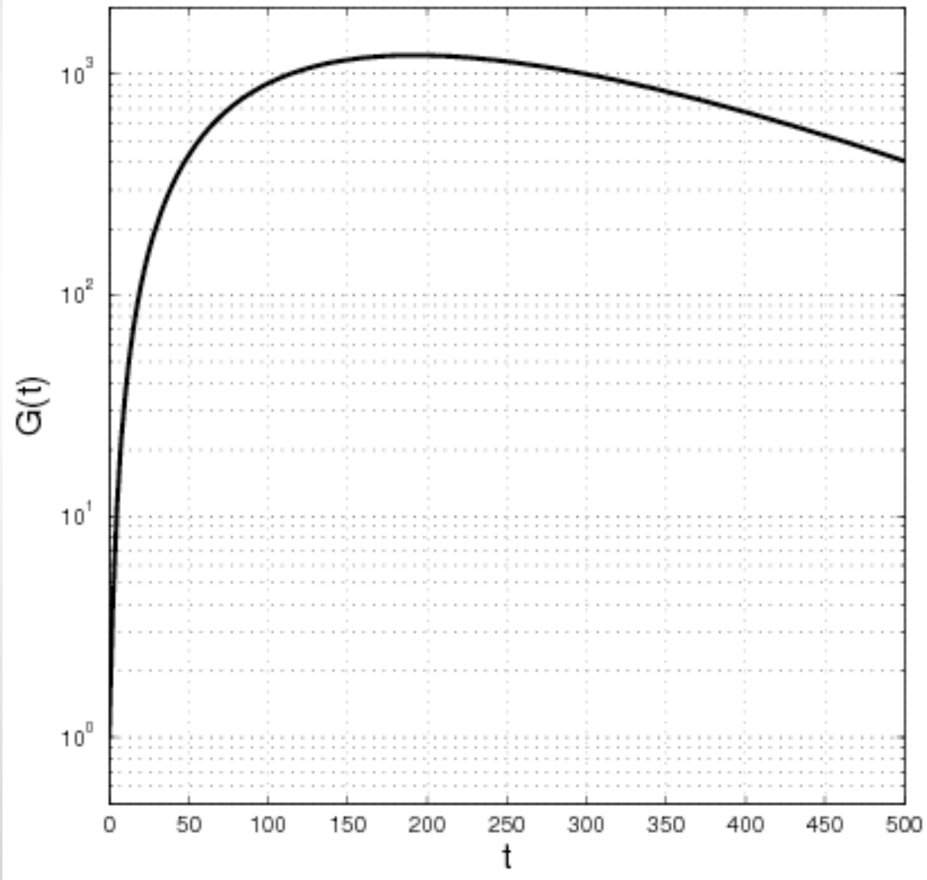

Example: plane Poiseuille flow

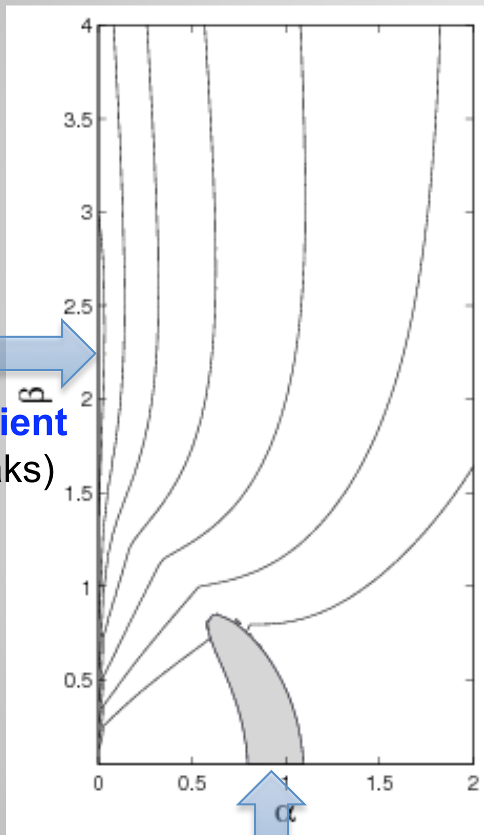

largest **transient** growth (streaks)

three-dimensional impulse response

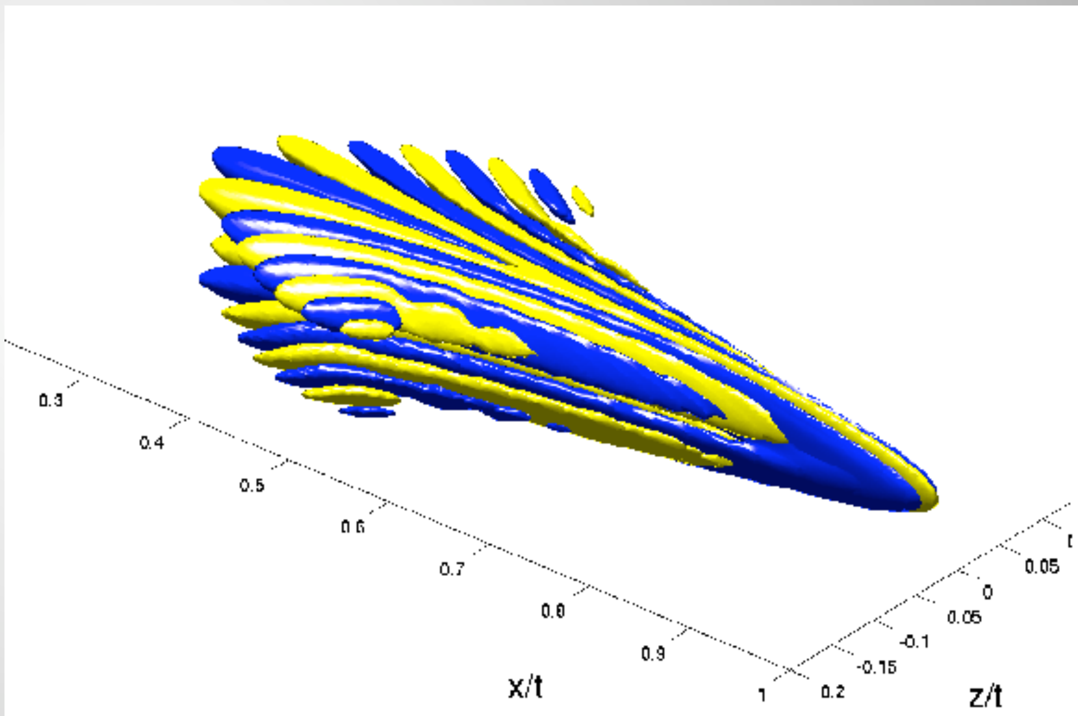

largest **exponential** growth (Tollmien-Schlichting wave)

Generalizations

time-periodic and generally time-dependent flow → pseudo-Floquet analysis
adjoint analysis

In many industrial applications (e.g., turbomachinery) the mean flow is periodic in time due to an oscillatory pressure gradient

We have

$$\frac{d}{dt} q = L(t) q \qquad L(t+T) = L(t)$$

period T

with the formal solution

$$\underbrace{q(t)}_{\text{final solution}} = \underbrace{A(t)}_{\text{propagator}} \underbrace{q_0}_{\text{initial condition}}$$

Generalizations

time-periodic and generally time-dependent flow ➡

pseudo-Floquet analysis
adjoint analysis

periodicity requires that

$$A(t+T) = A(t)\ A(T) = A(t)\, C$$

monodromy matrix
(mapping over one period)

$$q_n = C\ q_{n-1} = C^n\ q_0$$

initial state

Generalizations

time-periodic and generally time-dependent flow → pseudo-Floquet analysis, adjoint analysis

$$q_n = C\ q_{n-1} = C^n\ q_0$$

energy amplification from period to period

$$G_n^2 = \max_{q_0} \frac{\|q_n\|^2}{\|q_0\|^2} = \max_{q_0} \frac{\|C^n q_0\|^2}{\|q_0\|^2} = \|C^n\|^2$$

The eigenvalues of C are known as Floquet multipliers.

Question: Do the Floquet multipliers describe the behavior of $\|C^n\|^2$?

Generalizations

time-periodic and generally time-dependent flow → pseudo-Floquet analysis
adjoint analysis

as before, let us compute bounds

$$\rho^{2n} \leq \|C^n\|^2 \leq \kappa^2(S)\rho^{2n}$$

largest Floquet
multiplier

Conclusion: only for normal monodromy matrices does the largest Floquet multiplier describe the behavior from period to period

for nonnormal monodromy matrices there is a potential for transient amplification from period to period; only the asymptotic behavior $n \longrightarrow \infty$ is governed by the largest Floquet multiplier

Generalizations

time-periodic and generally time-dependent flow → pseudo-Floquet analysis
adjoint analysis

Example: pulsatile channel flow

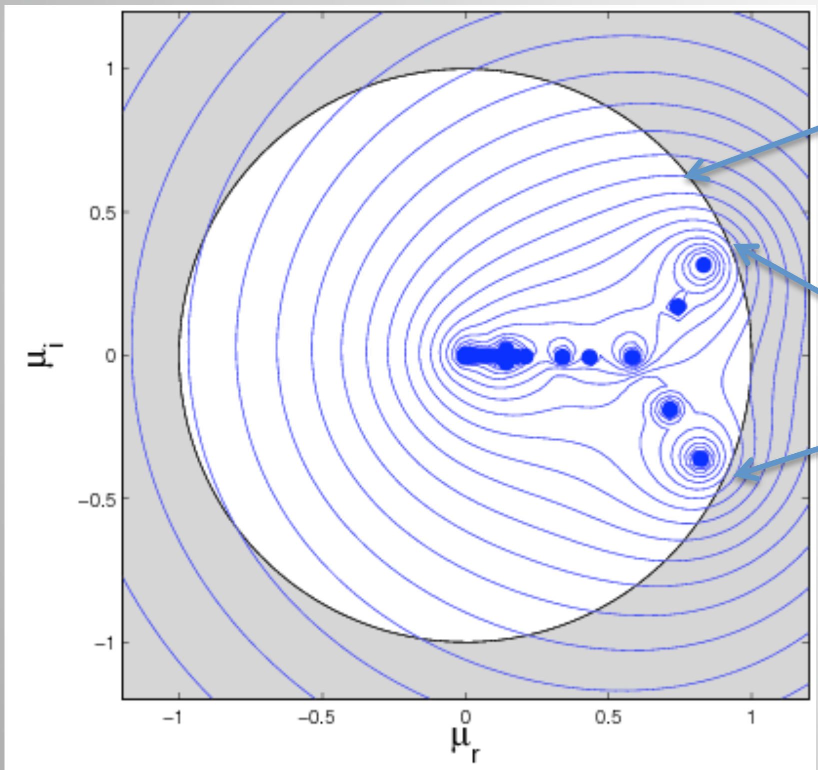

all Floquet multipliers are inside the unit disk indicating asymptotic stability (contractivity) as $n \longrightarrow \infty$

the resolvent contours reach outside the unit disk suggesting initial transient growth from period to period

Generalizations

time-periodic and generally time-dependent flow → pseudo-Floquet analysis
adjoint analysis

Example: pulsatile channel flow

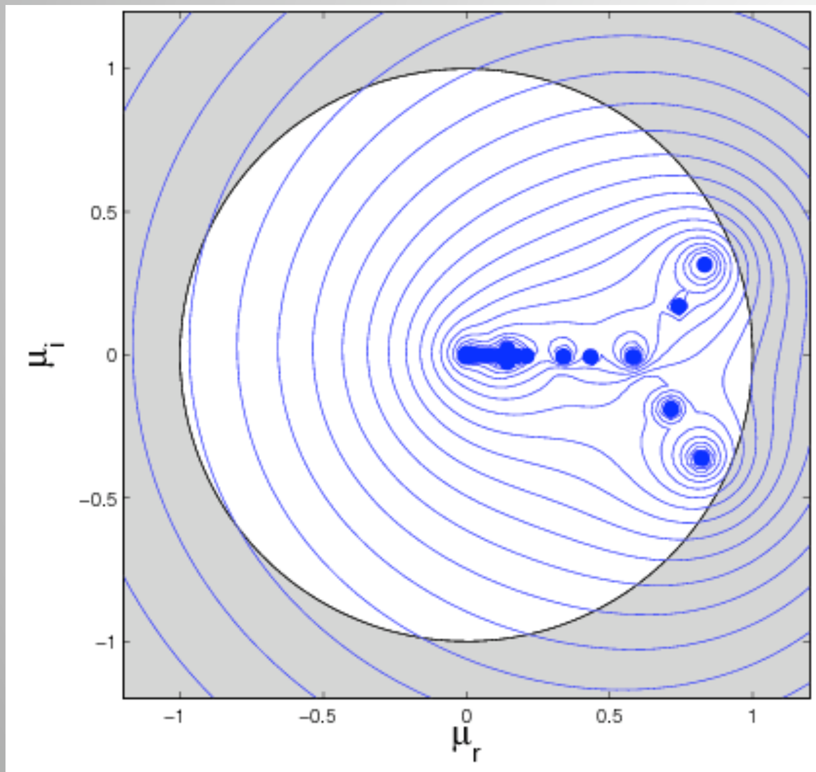

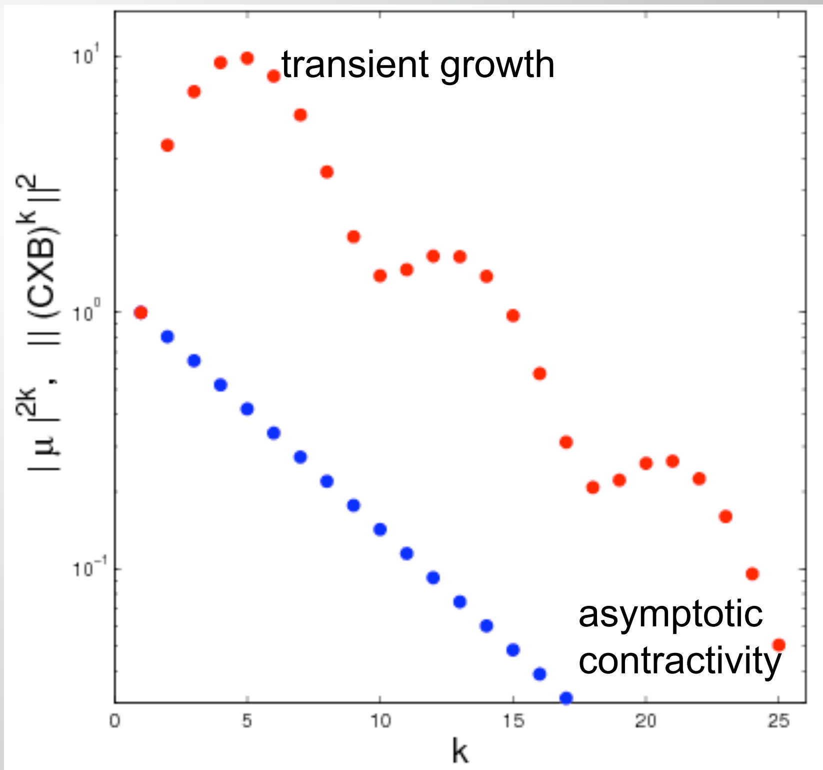

Generalizations

time-periodic and generally time-dependent flow → pseudo-Floquet analysis
adjoint analysis

Example: pulsatile channel flow

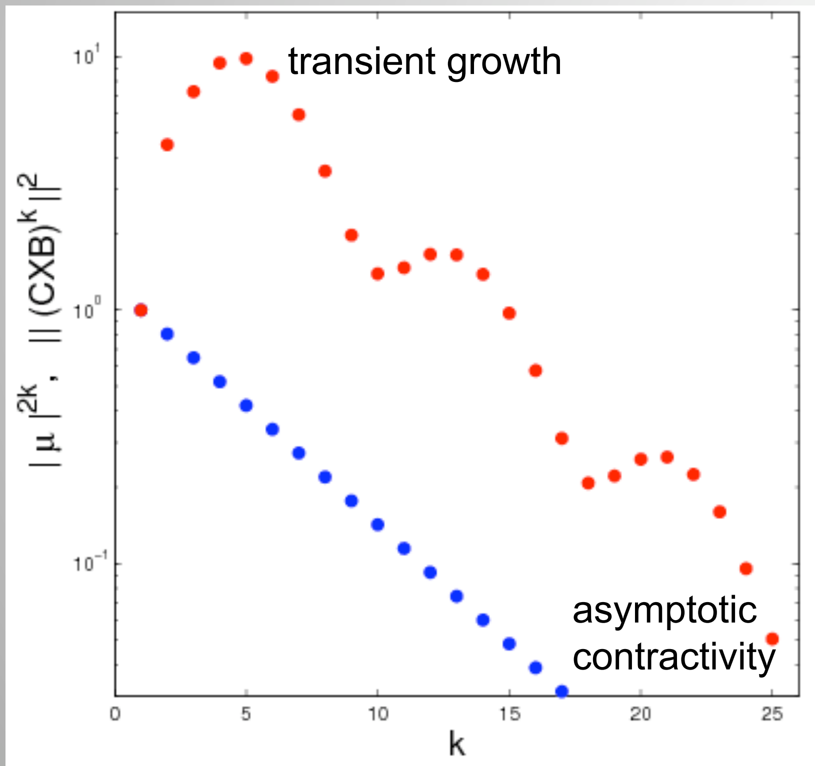

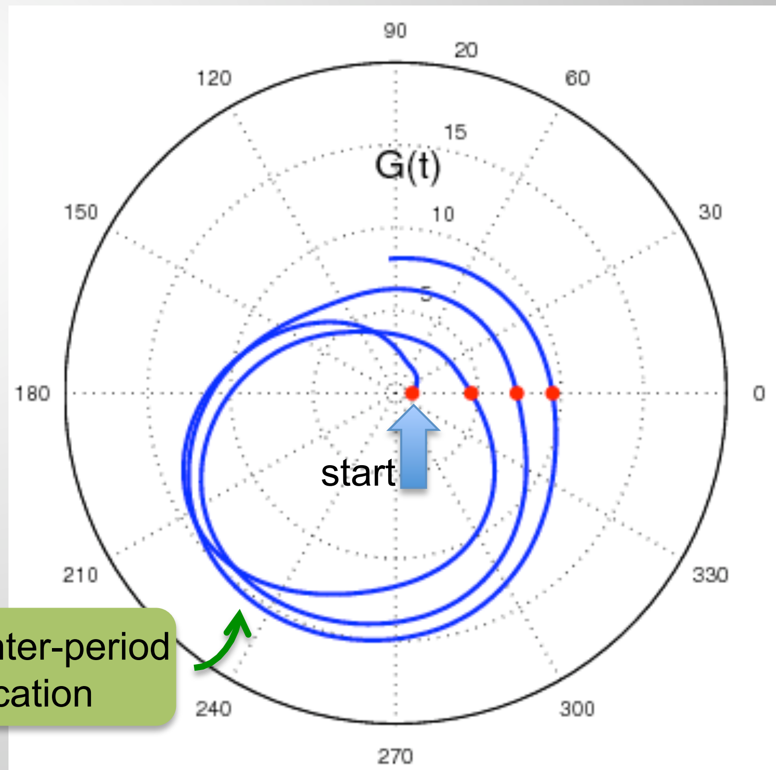

large inter-period amplification

Generalizations

time-periodic and generally time-dependent flow $\Rightarrow$ pseudo-Floquet analysis
adjoint analysis

Example: pulsatile channel flow

Can we analyze the amplification of energy between one period, i.e., for a non-periodic system matrix ?

We have
$$\frac{d}{dt} q = L(t) q$$

with the formal solution
$$\underbrace{q(t)}_{\text{final solution}} = \underbrace{A(t)}_{\text{propagator}} \; \underbrace{q_0}_{\text{initial condition}}$$

Generalizations

time-periodic and generally time-dependent flow → pseudo-Floquet analysis, adjoint analysis

Example: pulsatile channel flow

We can formulate the optimal amplification of energy as

$$G(t)^2 = \max_{q_0} \frac{\langle q, q \rangle}{\langle q_0, q_0 \rangle}$$

$$= \max_{q_0} \frac{\langle A(t) q_0, A(t) q_0 \rangle}{\langle q_0, q_0 \rangle}$$

$$= \max_{q_0} \frac{\langle A^H(t) A(t) q_0, q_0 \rangle}{\langle q_0, q_0 \rangle}$$

Generalizations

time-periodic and generally time-dependent flow ➡ pseudo-Floquet analysis
adjoint analysis

Example: pulsatile channel flow

$$G(t)^2 = \max_{q_0} \frac{\langle \boxed{A^H(t) A(t)} q_0, q_0 \rangle}{\langle q_0, q_0 \rangle}$$

$A^H A$ is a ***normal*** matrix

- the maximum is achieved for the principal eigenvector of $A^H A$
- the principal eigenvector (and eigenvalue) can be found by power iteration

$$q_0^{(n+1)} = \rho^{(n)} A^H A \; q_0^{(n)}$$

Generalizations

time-periodic and generally time-dependent flow → pseudo-Floquet analysis
adjoint analysis

Example: pulsatile channel flow

$$q_0^{(n+1)} = \rho^{(n)} A^H \boxed{A\ q_0^{(n)}}$$

break to power iteration into two pieces

first step

$$w(t) = A\ q_0^{(n)}$$

propagation of initial condition forward in time

Generalizations

time-periodic and generally time-dependent flow → pseudo-Floquet analysis
adjoint analysis

Example: pulsatile channel flow

$$q_0^{(n+1)} = \rho^{(n)} \boxed{A^H} A \; q_0^{(n)}$$

break to power iteration into two pieces

second step $$q_0^{(n+1)} = \rho^{(n)} A^H(t) w(t)$$

propagation of final condition backward in time

Generalizations

time-periodic and generally time-dependent flow → pseudo-Floquet analysis
adjoint analysis

Example: pulsatile channel flow

$$q_0^{(n+1)} = \rho^{(n)} A^H A \, q_0^{(n)}$$

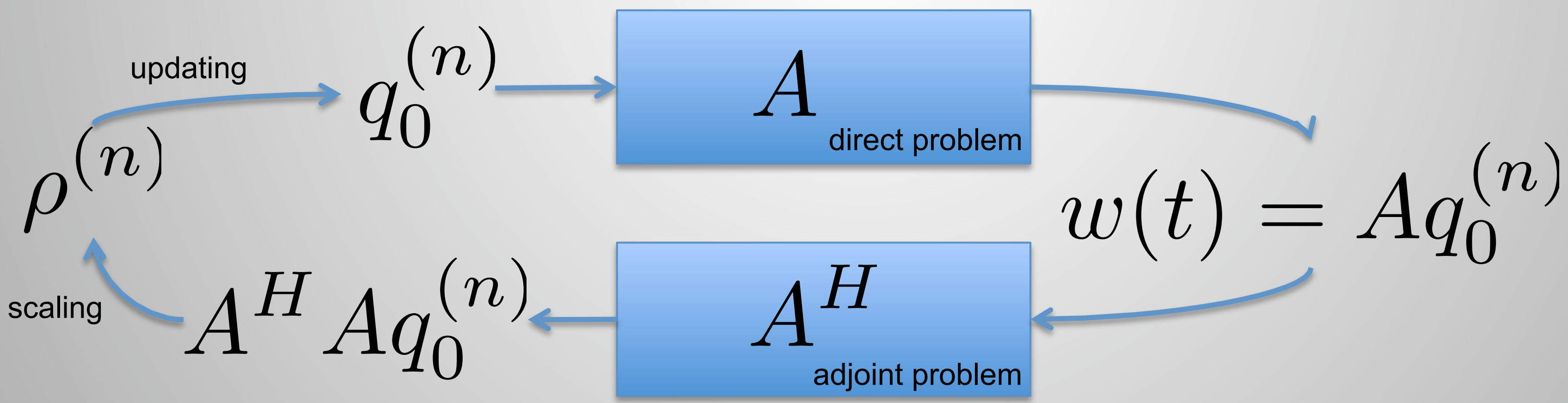

Generalizations

time-periodic and generally time-dependent flow → pseudo-Floquet analysis, adjoint analysis

Example: pulsatile channel flow

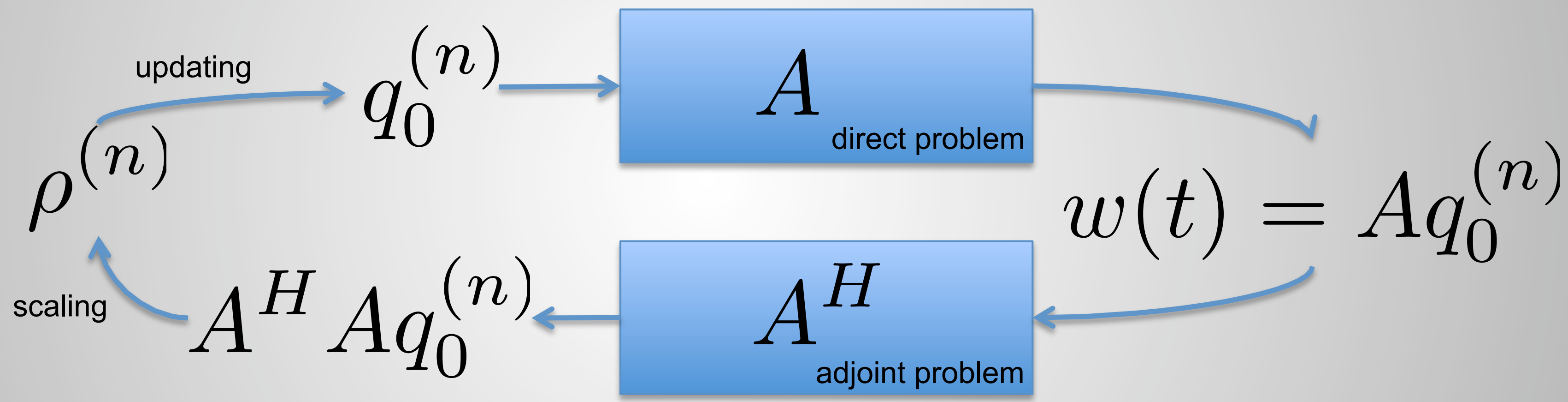

A can be any discretized solution operator. The above technique (adjoint looping) can be applied to general time-dependent stability problems.

Generalizations

time-periodic and generally time-dependent flow → pseudo-Floquet analysis
adjoint analysis

Example: pulsatile channel flow

applying adjoint looping to the pulsatile (inter-period) stability problem

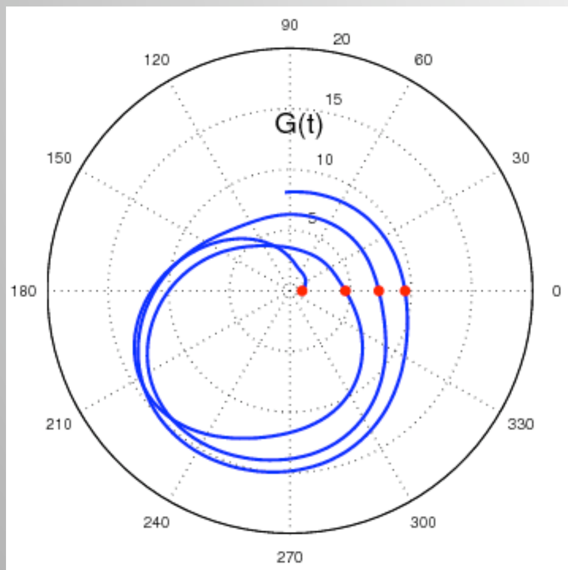

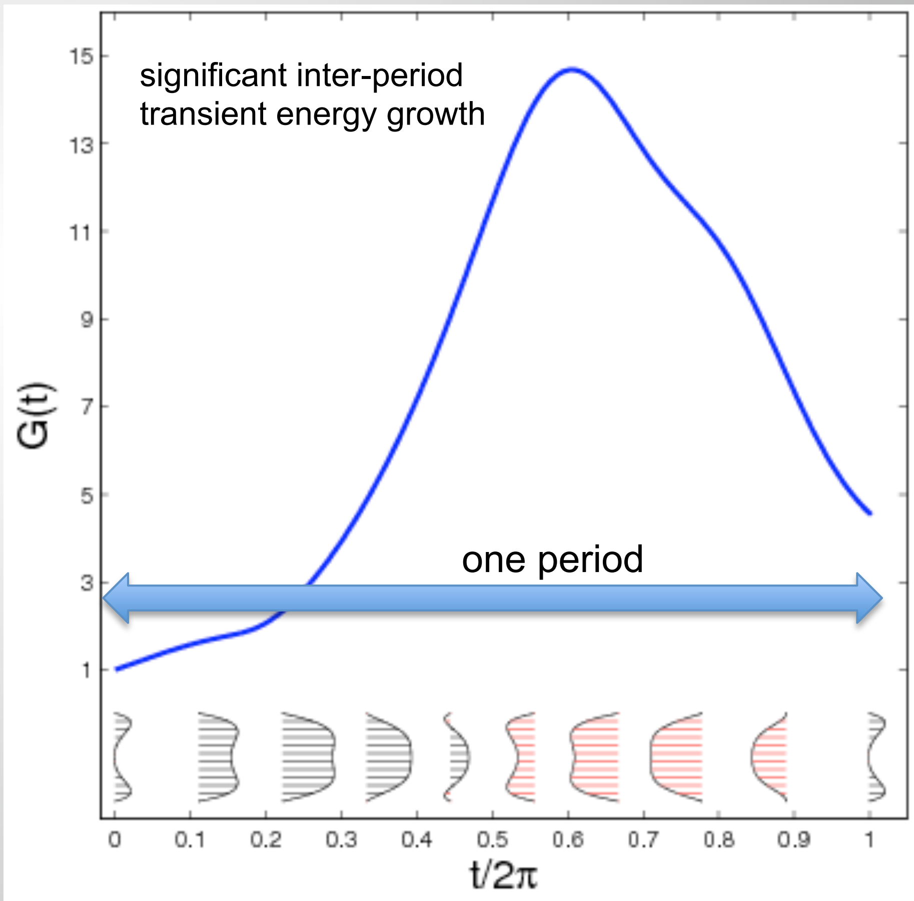

Generalizations

time-periodic and generally time-dependent flow → pseudo-Floquet analysis, adjoint analysis

Another look at the direct-adjoint system

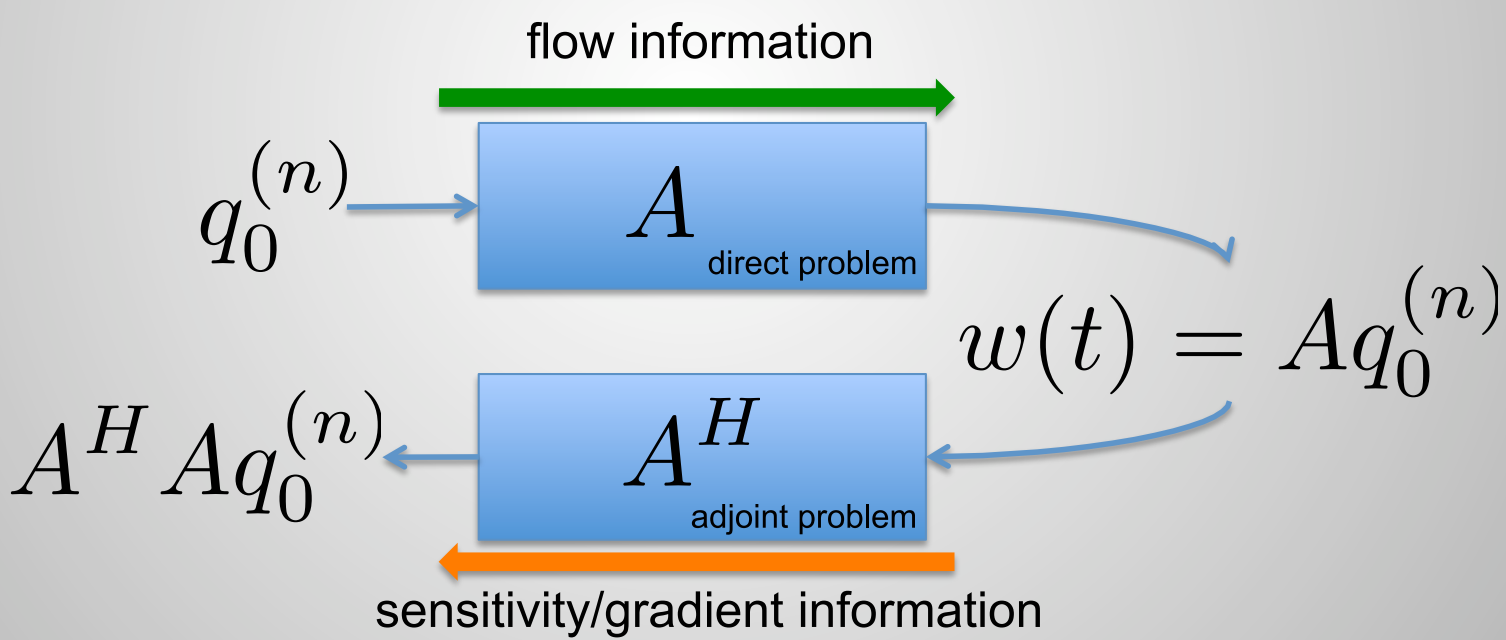

Generalizations

time-periodic and generally time-dependent flow → pseudo-Floquet analysis
adjoint analysis

reformulate the optimal growth problem variationally

we wish to optimize

$$J = \frac{||q||^2}{||q_0||^2} \rightarrow \max$$

subject to the constraint

$$\frac{d}{dt}q - Lq = 0$$

Generalizations

time-periodic and generally time-dependent flow → pseudo-Floquet analysis, adjoint analysis

rather than substituting the constraint directly into the cost functional …

$$J = \frac{\|q\|^2}{\|q_0\|^2} = \frac{\|\exp(tL)q_0\|^2}{\|q_0\|^2} \rightarrow \max$$

$$\frac{d}{dt}q - Lq = 0$$

Generalizations

time-periodic and generally time-dependent flow → pseudo-Floquet analysis
adjoint analysis

… we enforce the equation via a Lagrange multiplier $\tilde{q}$

$$J = \frac{||q||^2}{||q_0||^2} - \left\langle \tilde{q}, \left(\frac{d}{dt} q - Lq \right) \right\rangle \rightarrow \max$$

This has the advantage that the solution to the governing equation does not have to known explicitly.

Other constraints (such as initial and boundary conditions) can be added.

Generalizations

time-periodic and generally time-dependent flow $\Rightarrow$ pseudo-Floquet analysis
adjoint analysis

for an optimum we have to require all first variations of J to be zero

$$J = \frac{\|q\|^2}{\|q_0\|^2} - \left\langle \tilde{q}, \left(\frac{d}{dt} q - Lq \right) \right\rangle \to \max$$

$$\frac{\delta J}{\delta \tilde{q}} = 0 \quad \Rightarrow \quad \left\langle \delta\tilde{q}, \left(\frac{d}{dt} q - Lq \right) \right\rangle = 0$$

$$\frac{\delta J}{\delta q} = 0 \quad \Rightarrow \quad \left\langle \tilde{q}, \left(\frac{d}{dt} \delta q - L\, \delta q \right) \right\rangle = 0$$

Generalizations

time-periodic and generally time-dependent flow $\Rightarrow$ pseudo-Floquet analysis
adjoint analysis

for an optimum we have to require all first variations of J to be zero

$$J = \frac{\|q\|^2}{\|q_0\|^2} - \left\langle \tilde{q}, \left(\frac{d}{dt} q - Lq \right) \right\rangle \to \max$$

$$\frac{\delta J}{\delta \tilde{q}} = 0 \quad \Rightarrow \quad \boxed{\frac{d}{dt} q - Lq = 0}$$

$$\frac{\delta J}{\delta q} = 0 \quad \Rightarrow \quad \left\langle \tilde{q}, \left(\frac{d}{dt} \delta q - L\, \delta q \right) \right\rangle = 0$$

Generalizations

time-periodic and generally time-dependent flow → pseudo-Floquet analysis
adjoint analysis

for an optimum we have to require all first variations of J to be zero

$$J = \frac{\|q\|^2}{\|q_0\|^2} - \left\langle \tilde{q}, \left(\frac{d}{dt} q - Lq \right) \right\rangle \to \max$$

$$\frac{\delta J}{\delta \tilde{q}} = 0 \quad \Rightarrow \quad \boxed{\frac{d}{dt} q - Lq = 0}$$ direct problem

$$\frac{\delta J}{\delta q} = 0 \quad \Rightarrow \quad \boxed{-\frac{d}{dt} \tilde{q} - L^H \tilde{q} = 0}$$ adjoint problem

Generalizations

time-periodic and generally time-dependent flow ➡ pseudo-Floquet analysis
adjoint analysis

adjoint variables can be interpreted as sensitivities

$$J = \mathrm{obj} - \left\langle \tilde{q}, \left(\frac{d}{dt} q - Lq \right) \right\rangle \to \max$$

let us add an external body force to the governing equations

$$\frac{d}{dt} q - Lq = f$$

external force

$$\boxed{\nabla_f J = -\tilde{q}}$$

sensitivity to external body force

Generalizations

time-periodic and generally time-dependent flow → pseudo-Floquet analysis, adjoint analysis

Example: which adjoint variable measures the sensitivity to a mass source/sink?

$$J = \mathrm{obj} - \underbrace{\langle \tilde{\mathbf{u}}, NS(\mathbf{u}) \rangle}_{\text{enforcing momentum conservation}} - \underbrace{\langle \xi, \nabla \cdot \mathbf{u} \rangle}_{\text{enforcing mass conservation}}$$

$$-\langle \xi, \nabla \cdot \mathbf{u} \rangle \xrightarrow[\text{by parts}]{\text{integration}} \langle \nabla \xi, \delta \mathbf{u} \rangle$$

ξ is the adjoint pressure

Generalizations

time-periodic and generally time-dependent flow → pseudo-Floquet analysis
adjoint analysis

Example: which adjoint variable measures the sensitivity to a mass source/sink?

$$J = \mathrm{obj} - \langle \tilde{\mathbf{u}}, NS(\mathbf{u}) \rangle - \langle \xi, \nabla \cdot \mathbf{u} \rangle$$

enforcing momentum conservation

enforcing mass conservation

assuming a mass source/sink

$$\nabla \cdot \mathbf{u} = Q$$

$$\delta J = \langle \xi, \delta Q \rangle$$

adjoint pressure = sensitivity to a mass source/sink

Generalizations

time-periodic and generally time-dependent flow → pseudo-Floquet analysis, adjoint analysis

for the incompressible Navier-Stokes equations

forcing | sensitivity

$$\frac{\partial \mathbf{u}}{\partial t} + \mathrm{advdiff}(\mathbf{U}, \mathbf{u}) + \nabla p = \mathbf{F} \qquad \nabla_{\mathbf{F}} J = \tilde{\mathbf{u}}$$

$$\nabla \cdot \mathbf{u} = Q \qquad \nabla_Q J = \tilde{p}$$

$$\mathbf{u} = \mathbf{u}_w \quad \text{on} \quad y = 0 \qquad \nabla_{\mathbf{u}_w} J = \tilde{\sigma}\big|_w$$

Generalizations

Sensitivity to internal changes
(changes of specific eigenvalues with respect to parameter variations)

general formulation

$$A(p)q = \lambda B q$$

p Reynolds number Re
wave number α, β
base-flow $U(y)$

perturbation expansion

$$(A + \delta A)(q + \delta q) = (\lambda + \delta\lambda) B (q + \delta q)$$

Generalizations

Sensitivity to internal changes
(changes of specific eigenvalues with respect to parameter variations)

general formulation

$$A(p)q = \lambda B q \qquad\qquad p$$

Reynolds number Re
wave number α, β
base-flow $U(y)$

perturbation expansion

$$\underbrace{(A-\lambda B)q}_{0} + (A-\lambda B)\delta q + (\delta A - \delta\lambda B)q + \underbrace{(\delta A - \delta\lambda B)\delta q}_{\approx 0} = 0$$

(higher order)

Generalizations

Sensitivity to internal changes
(changes of specific eigenvalues with respect to parameter variations)

general formulation

$$A(p)q = \lambda B q$$

p — Reynolds number Re
wave number α, β
base-flow $U(y)$

perturbation expansion

$$q^{+}\underset{0}{(A - \lambda B)}\delta q + q^{+}(\delta A - \delta\lambda B)q \approx 0$$

$$q^{+}(A - \lambda B) = 0 \quad \Leftrightarrow \quad (A^{+} - \lambda^{*} B^{+})q^{+} = 0$$

Generalizations

Sensitivity to internal changes
(changes of specific eigenvalues with respect to parameter variations)

general formulation

$$A(p)q = \lambda B q$$

p Reynolds number Re
wave number α, β
base-flow $U(y)$

perturbation expansion

$$\delta\lambda = \frac{q^+ \delta A q}{q^+ B q}$$

gradient

$$\nabla_p \lambda = \frac{q^+ \nabla_p A q}{q^+ B q}$$

Generalizations

Example: sensitivity to a scalar parameter

complex Ginzburg-Landau

$$u_t = \underbrace{\left(-\nu\partial_x + \gamma\partial_{xx} + \mu(x)\right)}_{A} u$$

$$\nu = U + 2ic_u$$

$$\nabla_U A = -\partial_x$$

eigenvalue sensitivity

$$\nabla_U \lambda = \tilde{u}^+ \nabla_U A \tilde{u}$$

$$A\tilde{u} = \lambda\tilde{u}$$

$$A^+\tilde{u}^+ = \lambda^*\tilde{u}^+$$

$$\lambda = \sigma + i\omega$$

$$\nabla_U \sigma = \mathrm{Real}(\nabla_U \lambda)$$

sensitivity of growth rate

$$\nabla_U \omega = \mathrm{Imag}(\nabla_U \lambda)$$

sensitivity of frequency

Generalizations

Sensitivity to internal changes
(changes of specific eigenvalues with respect to parameter variations)

Example: choose base flow profile as control variable

p Reynolds number Re
wave number α, β
$\boxed{\text{base-flow } U(y)}$

$$\nabla_{\mathbf{U}} \lambda = -(\nabla \mathbf{u})^H \tilde{\mathbf{u}} + \nabla \tilde{\mathbf{u}} \cdot \mathbf{u}^*$$

relate mean flow modification to small control forces

delay onset of instabilities to higher Reynolds numbers; increase stability margins

Generalizations

Flow chart for sensitivity/receptivity analysis

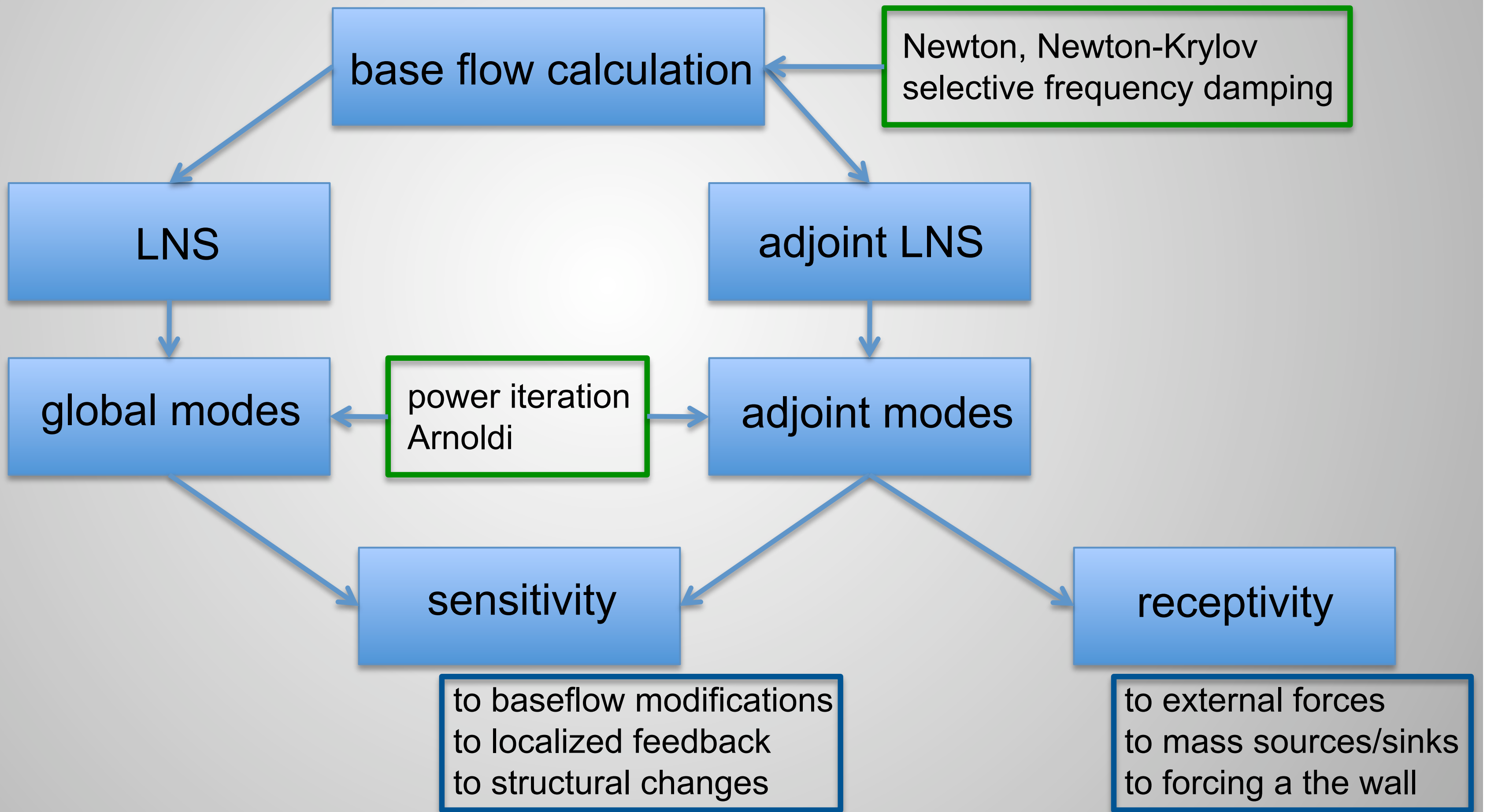

Generalizations

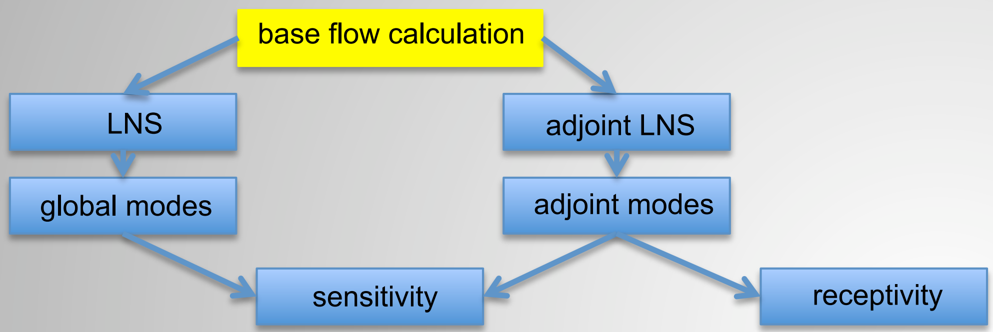

Example: flow around a cylinder

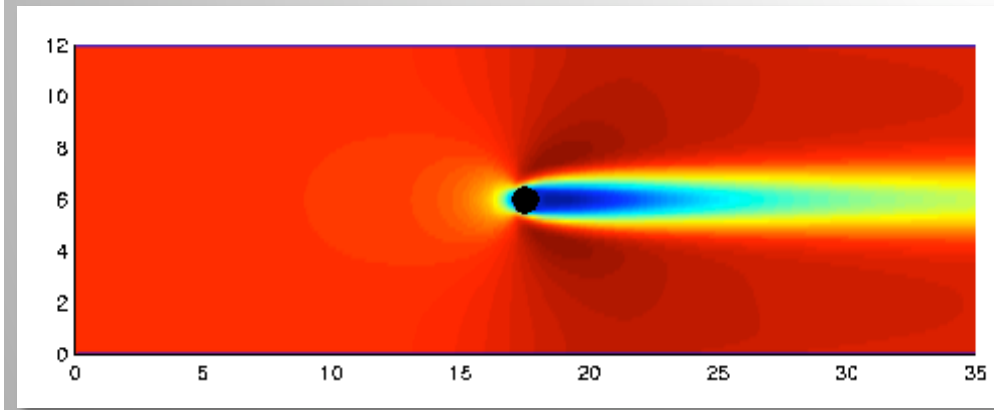

U_{base}

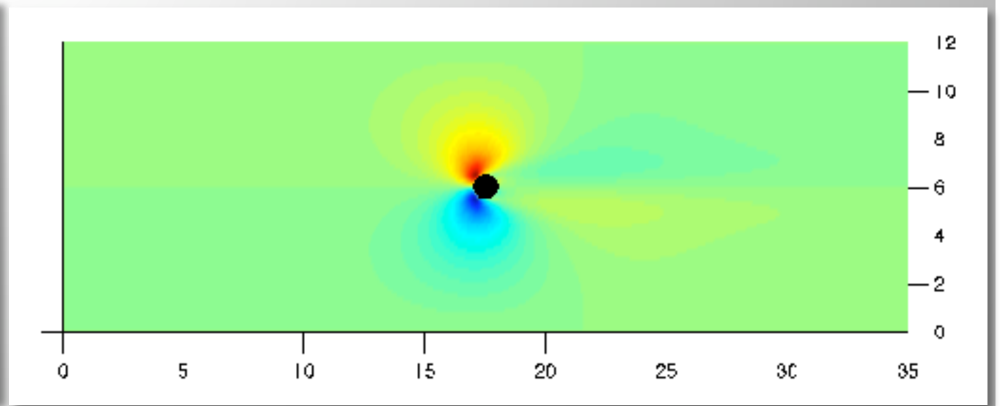

V_{base}

Generalizations

Example: flow around a cylinder

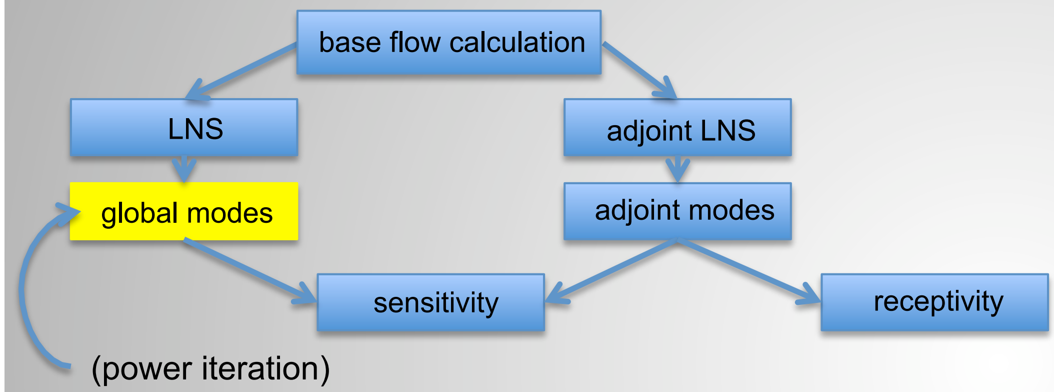

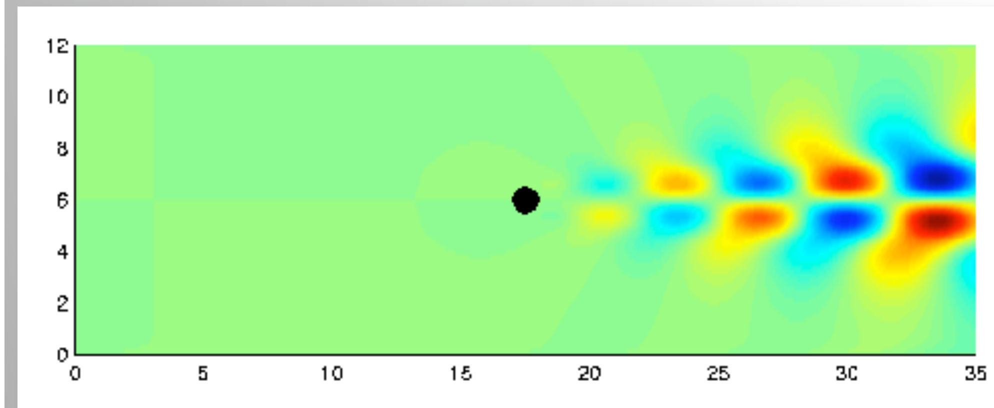

$$\tilde{u}_{\mathrm{direct}}$$

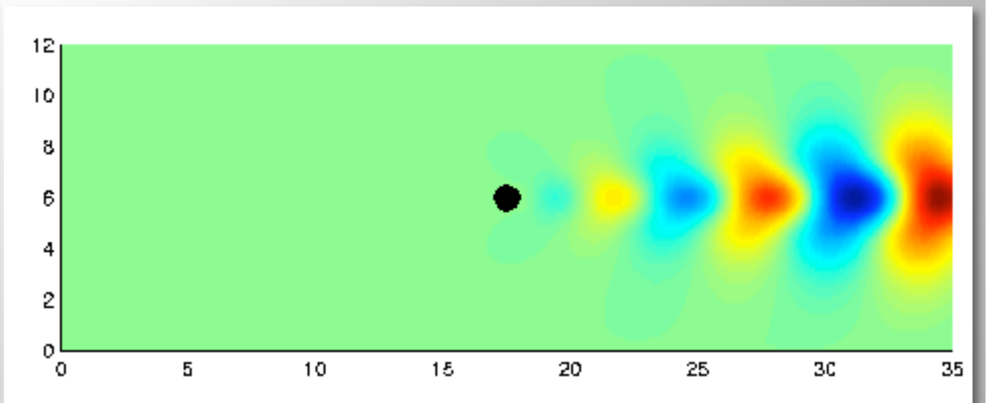

$$\tilde{v}_{\mathrm{direct}}$$

Generalizations

Example: flow around a cylinder

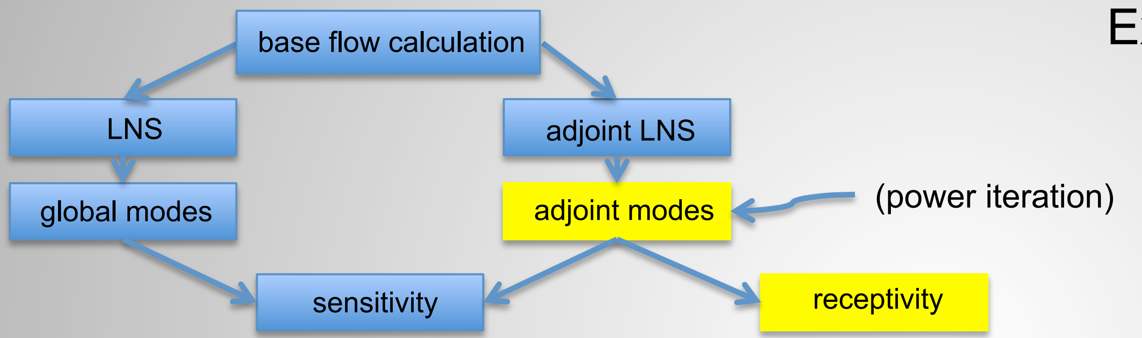

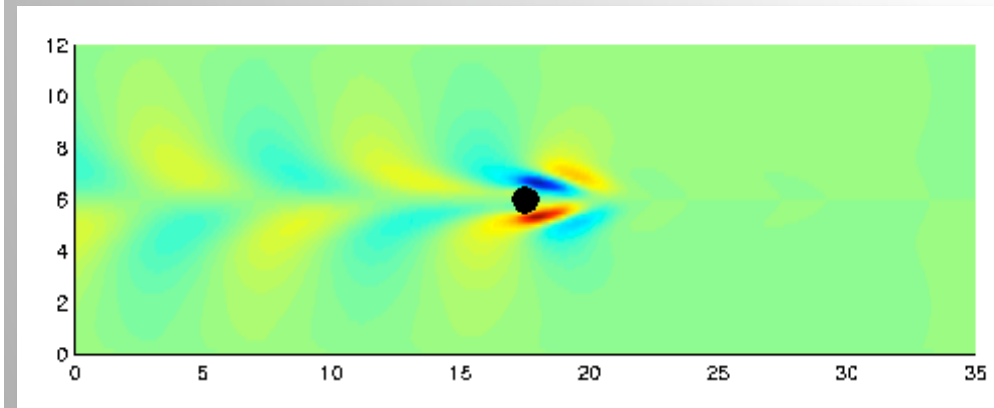

$\tilde{u}_{\text{adjoint}}$

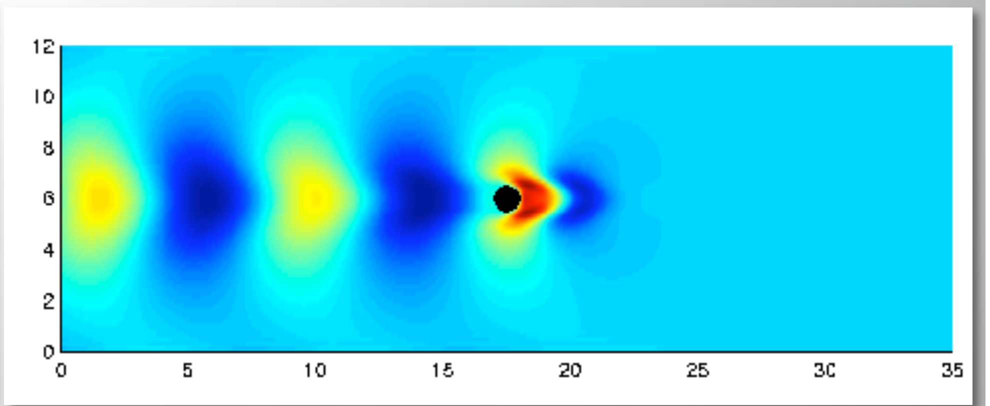

$\tilde{v}_{\text{adjoint}}$

Generalizations

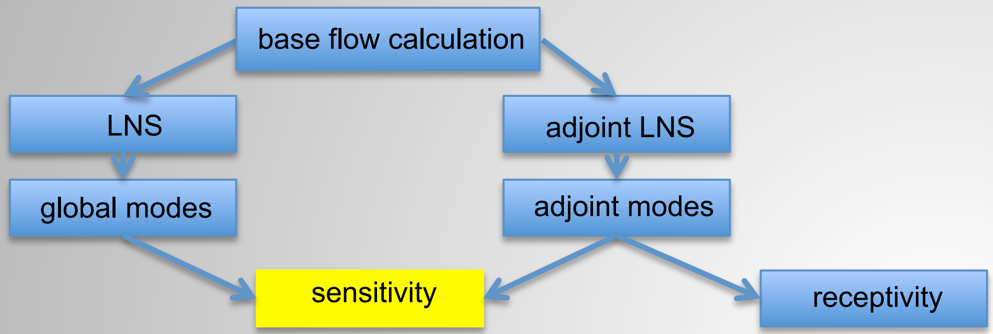

Example: flow around a cylinder

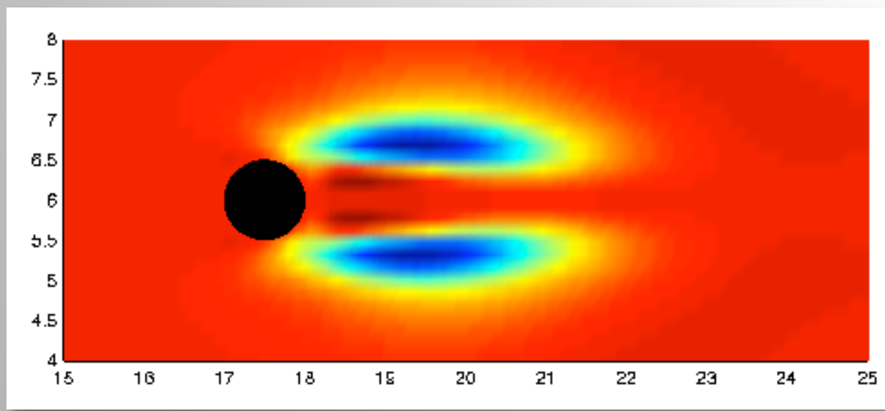

$u_{\text{wavemaker}}$

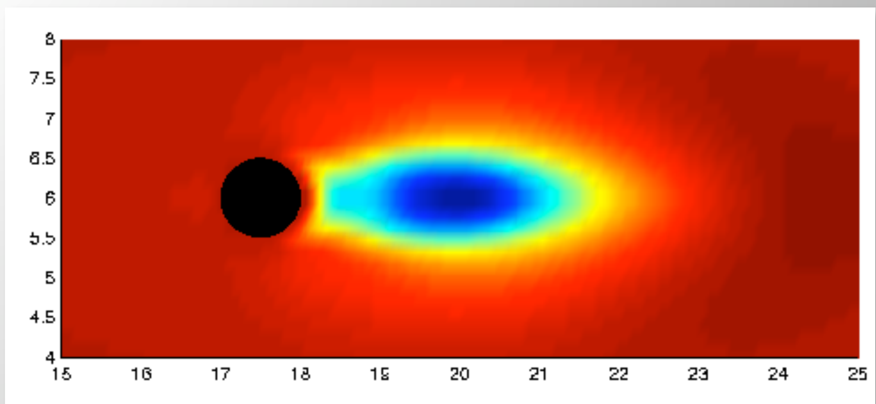

$v_{\text{wavemaker}}$

Generalizations

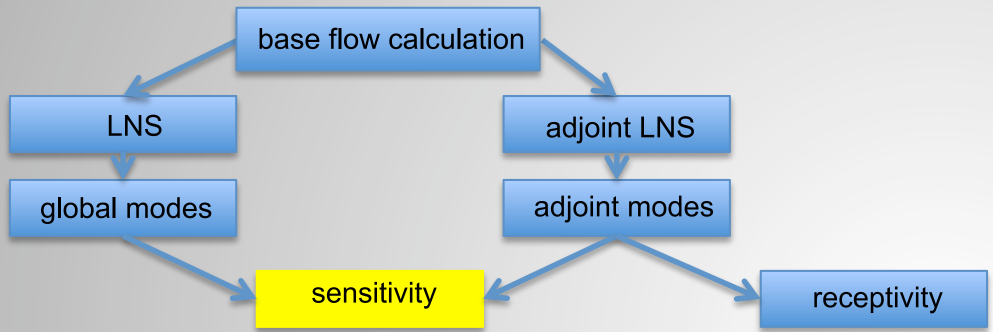

Example: flow around a cylinder

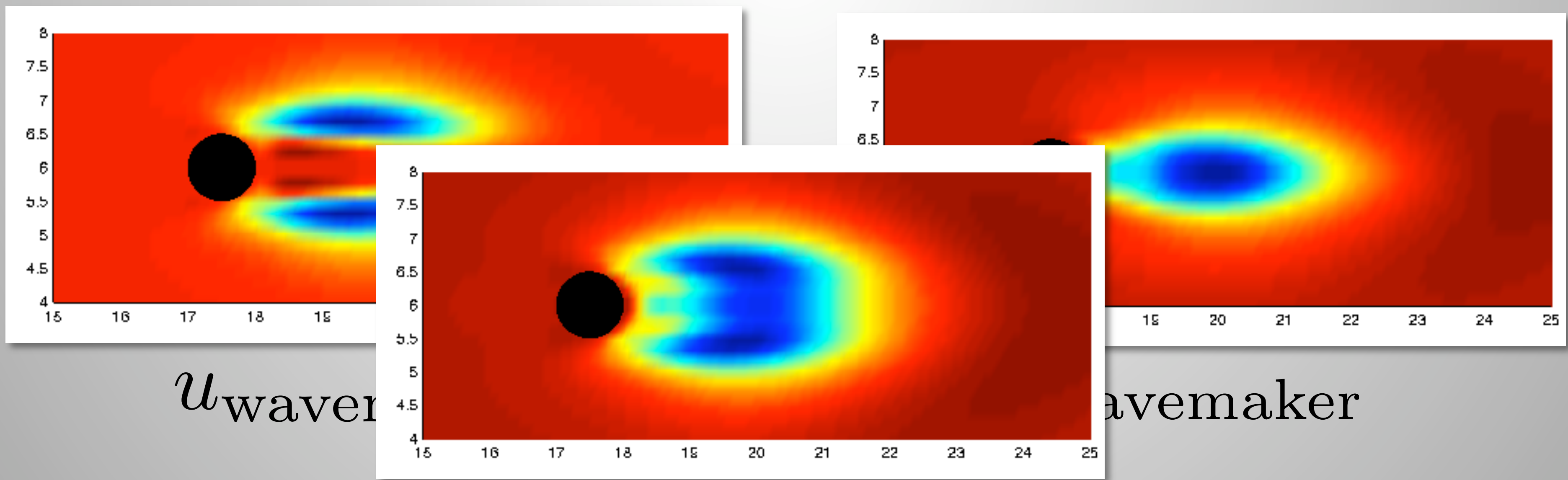

sensitivity to localized spatial feedback

Generalizations

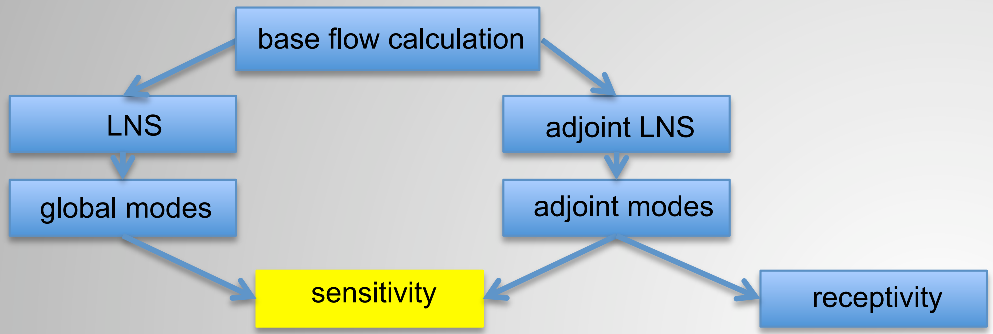

Example: flow around a cylinder

$$\nabla_{\mathbf{U}}\lambda = -(\nabla \mathbf{u})^{H}\tilde{\mathbf{u}} + \nabla\tilde{\mathbf{u}} \cdot \mathbf{u}^{*}$$

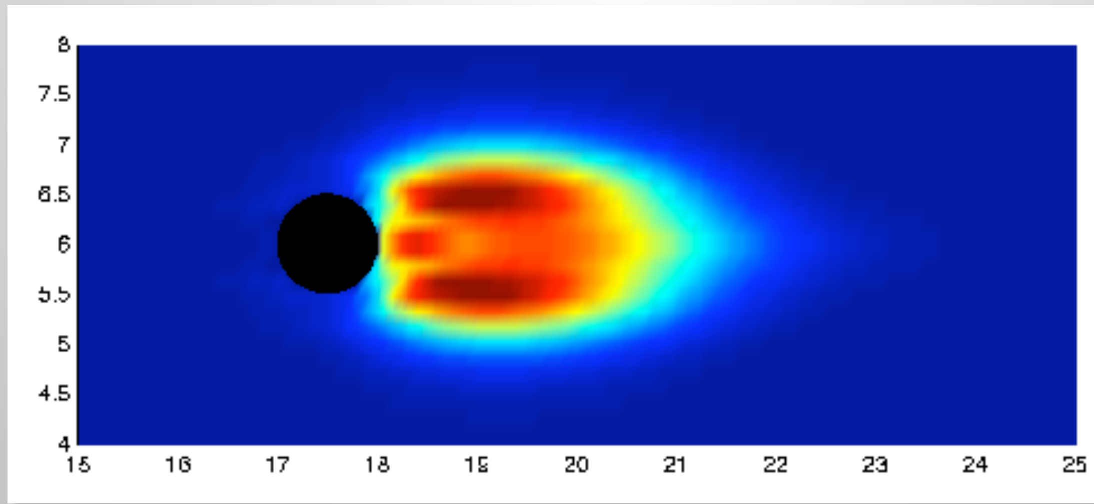

structural sensitivity

Generalizations

nonlinear perturbation dynamics → adjoint analysis with check-pointing

the variational formulation also allows us to add ***nonlinear*** constraints to the cost functional

$$J = \mathrm{obj} - \left\langle \tilde{q}, \left(\frac{d}{dt} q - N(q) \right) \right\rangle \rightarrow \max$$

nonlinear Navier-Stokes equations

How does this affect the adjoint looping ?

Generalizations

nonlinear perturbation dynamics $\Rightarrow$ adjoint analysis with check-pointing

Example: nonlinear advective terms

$$\langle \tilde{\mathbf{u}}, \mathbf{u}\nabla\mathbf{u} \rangle \xrightarrow{\text{first variation}} \langle -\mathbf{u}\nabla\tilde{\mathbf{u}}, \delta\mathbf{u} \rangle$$

We have **direct** terms appearing in the **adjoint** equation.

Generalizations

nonlinear perturbation dynamics → adjoint analysis with check-pointing

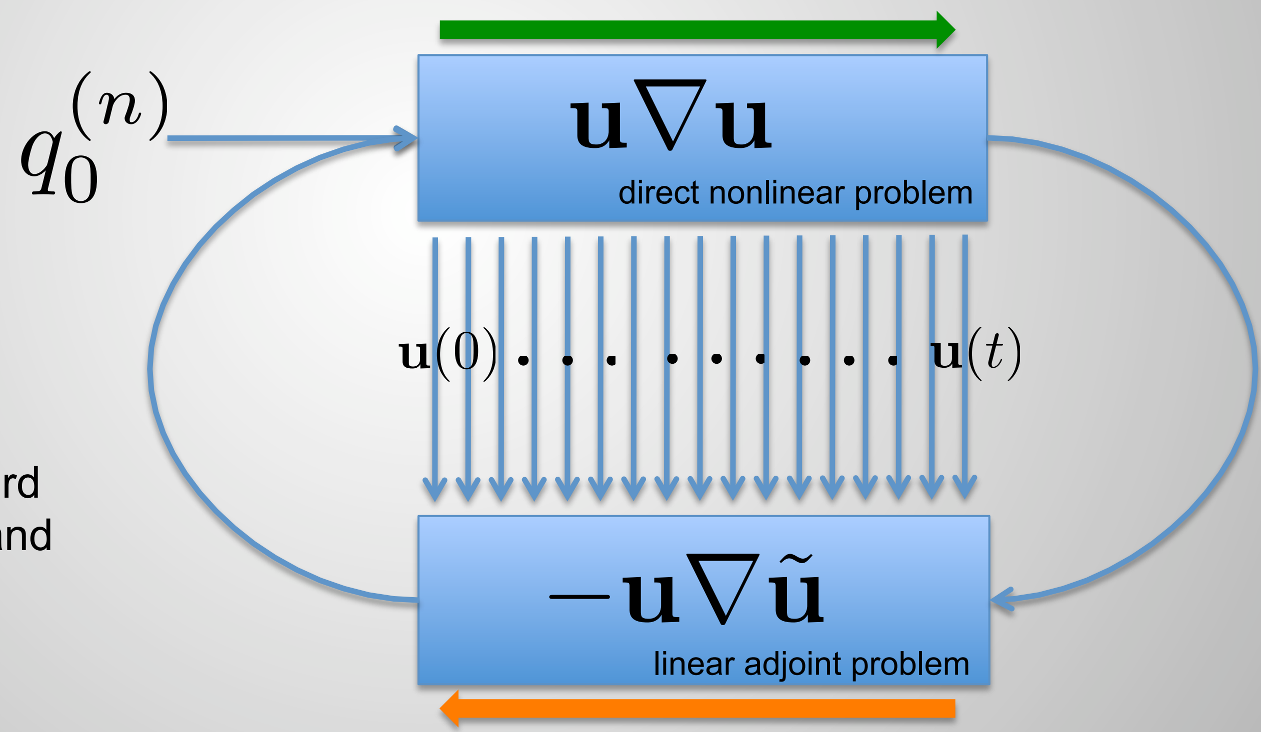

<u>checkpointing</u>

the flow fields at the forward sweep have to be saved and injected into the backward sweep

Generalizations

nonlinear perturbation dynamics → adjoint analysis with check-pointing

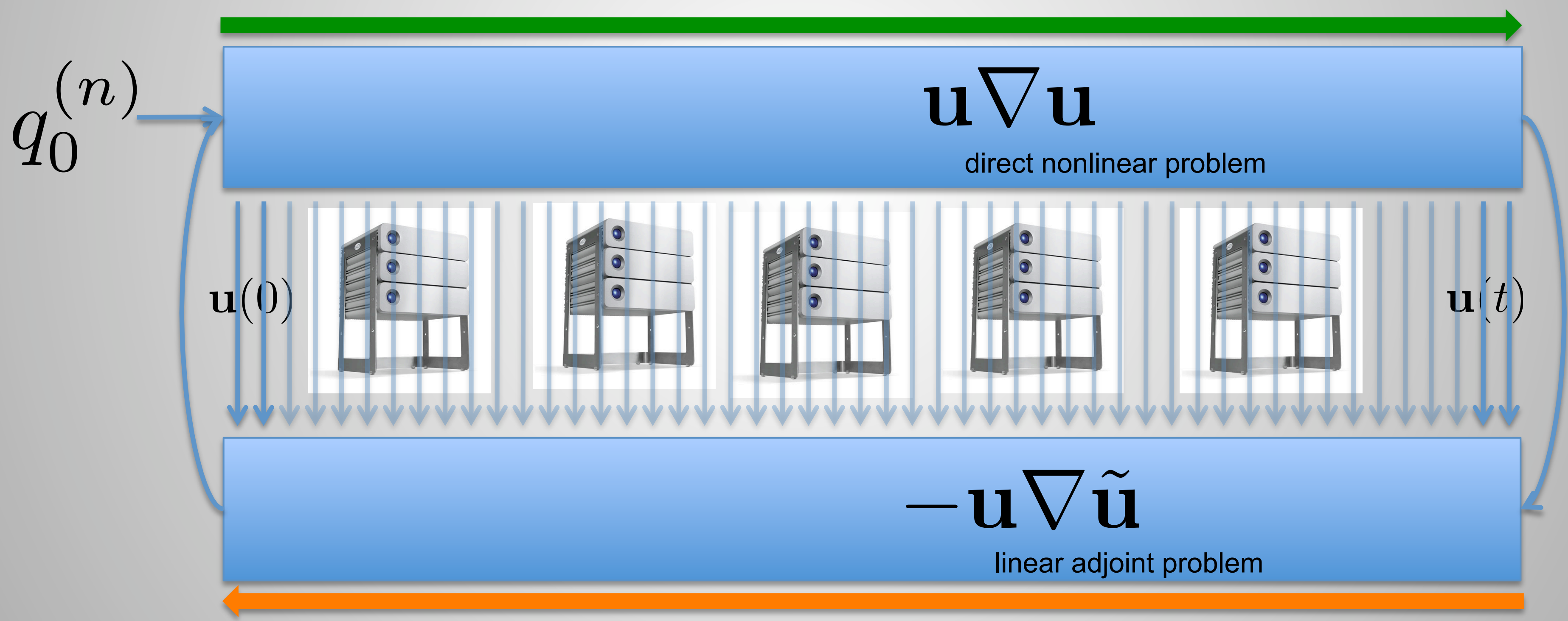

For long-time integrations and high-dimensional problems we quickly reach the limits of storage devices.

Generalizations

nonlinear perturbation dynamics ➡ adjoint analysis with check-pointing

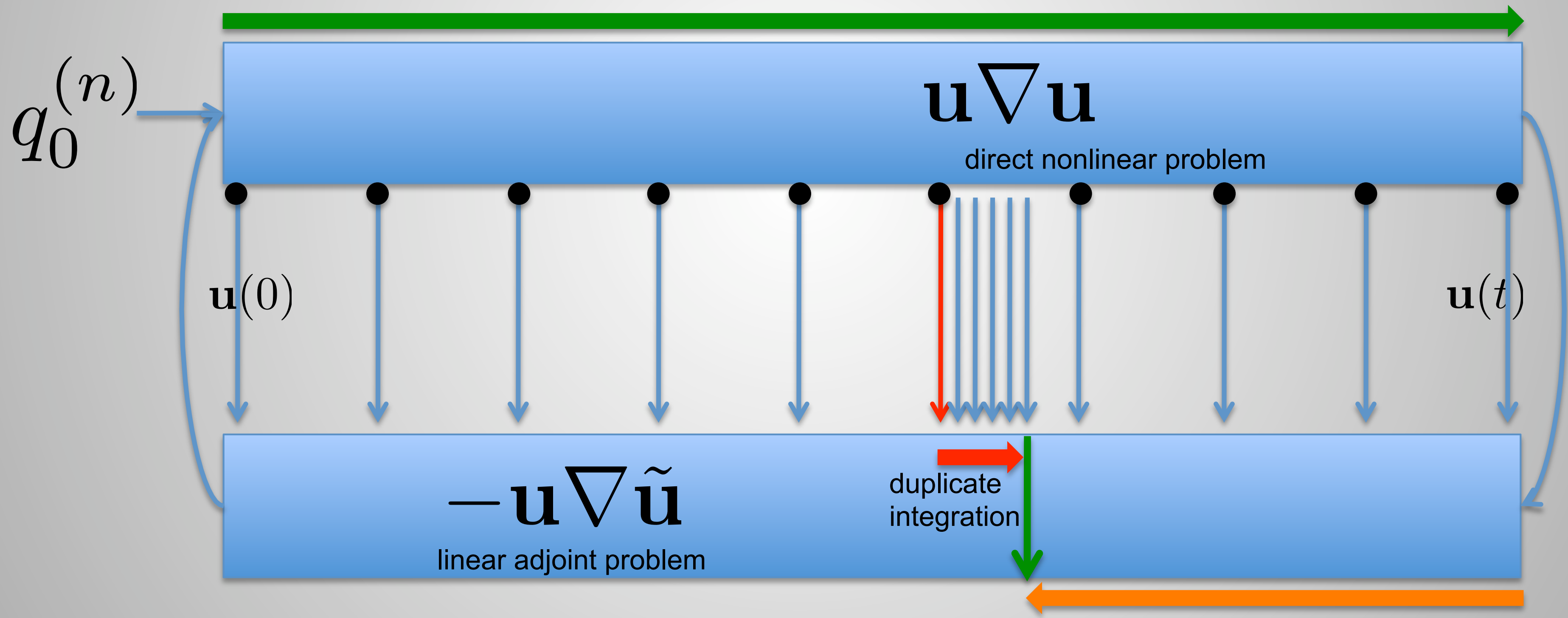

optimized checkpointing

store flow fields at coarse intervals ●●● and use as initial conditions for repeated forward integrations

Generalizations

multiple inhomogeneous directions/complex geometry → global mode analysis

for most industrial applications we cannot assume the existence of homogeneous directions that can be treated by a Fourier transform

rather, the eigenfunction will depend on more than one inhomogeneous coordinate direction

Generalizations

multiple inhomogeneous directions/complex geometry ⇒ global mode analysis

one inhomogeneous direction		two inhomogeneous directions
$q = \begin{pmatrix} q_1 \\ q_2 \\ \vdots \\ q_N \end{pmatrix}$	state vector	$q = \begin{pmatrix} q_{1,1} \\ q_{1,2} \\ \vdots \\ q_{N,N} \end{pmatrix}$
$L \in \mathbb{C}^{N \times N}$	stability matrix	$L \in \mathbb{C}^{N^2 \times N^2}$
$\sim N^3$	operation count	$\sim N^6$

Generalizations

multiple inhomogeneous directions/complex geometry ➡ global mode analysis

➡ direct eigenvalue algorithms quickly become prohibitively expensive

➡ iterative eigenvalue algorithms (Arnoldi technique) have to be used

Generalizations

multiple inhomogeneous directions/complex geometry $\Rightarrow$ global mode analysis

Arnoldi algorithm

action of the linear operator L is expressed within an orthonormal basis V

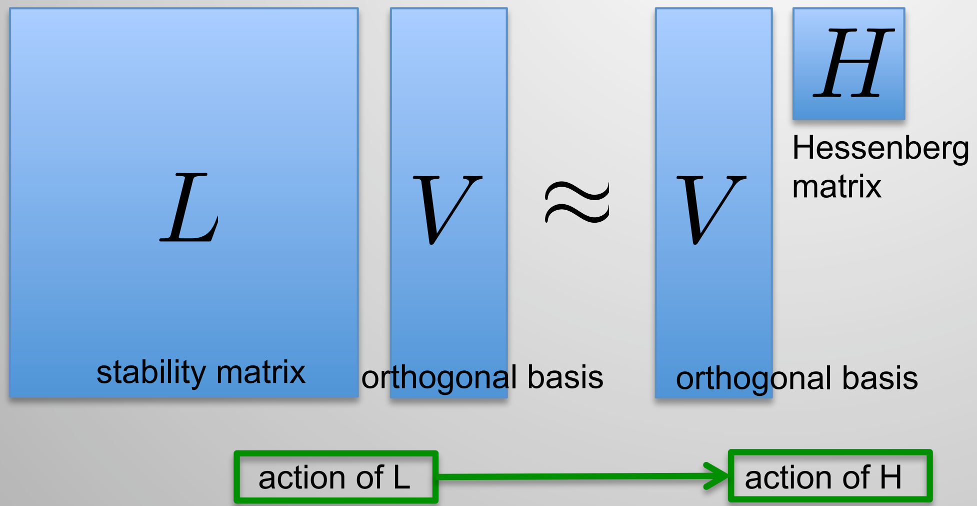

Generalizations

multiple inhomogeneous directions/complex geometry ➔ global mode analysis

Arnoldi algorithm

represent the (large) stability matrix by a low-rank approximation based on an orthogonal basis

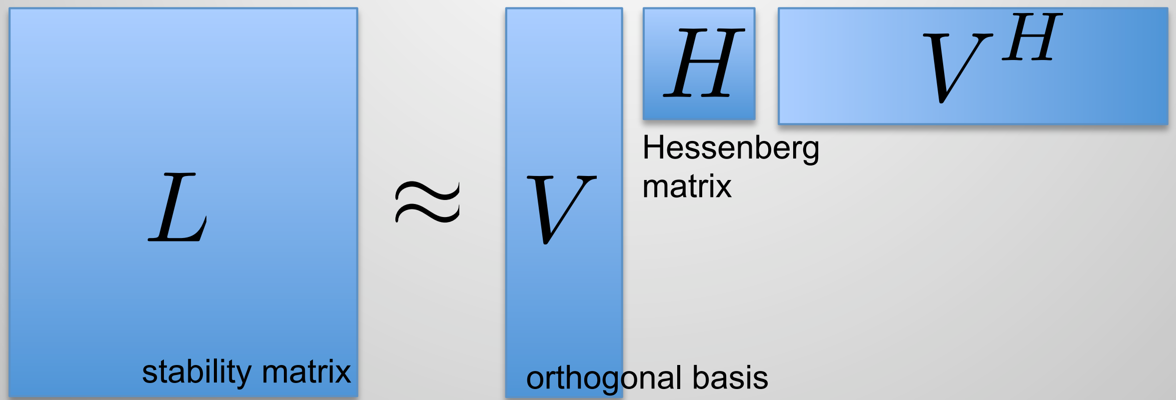

Generalizations

multiple inhomogeneous directions/complex geometry → global mode analysis

$$q_k = L\ q_{k-1}$$
$$\text{for} \quad j = 1 : k-1$$
$$H_{j,k-1} = \langle q_j\,, q_k \rangle$$
$$q_k = q_k - H_{j,k-1}\ q_j$$
$$\text{end}$$
$$H_{k,k-1} = \|q_k\|$$
$$q_k = q_k / H_{k,k-1}$$

only multiplications by L are necessary

$$\Rightarrow \quad \text{eig}\{L\} \approx \text{eig}\{H\}$$

Generalizations

multiple inhomogeneous directions/complex geometry → global mode analysis

computing global modes by diagonalizing $H = D\Lambda D^{-1}$

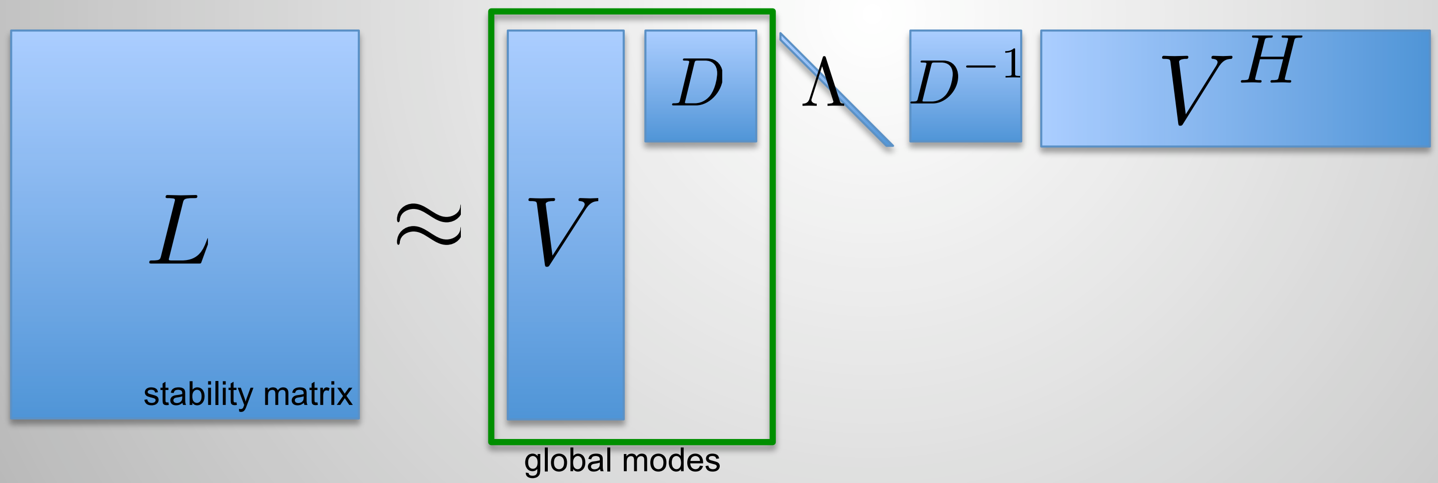

Generalizations

multiple inhomogeneous directions/complex geometry → global mode analysis

Examples of global modes: open cavity flow (two-dimensional)

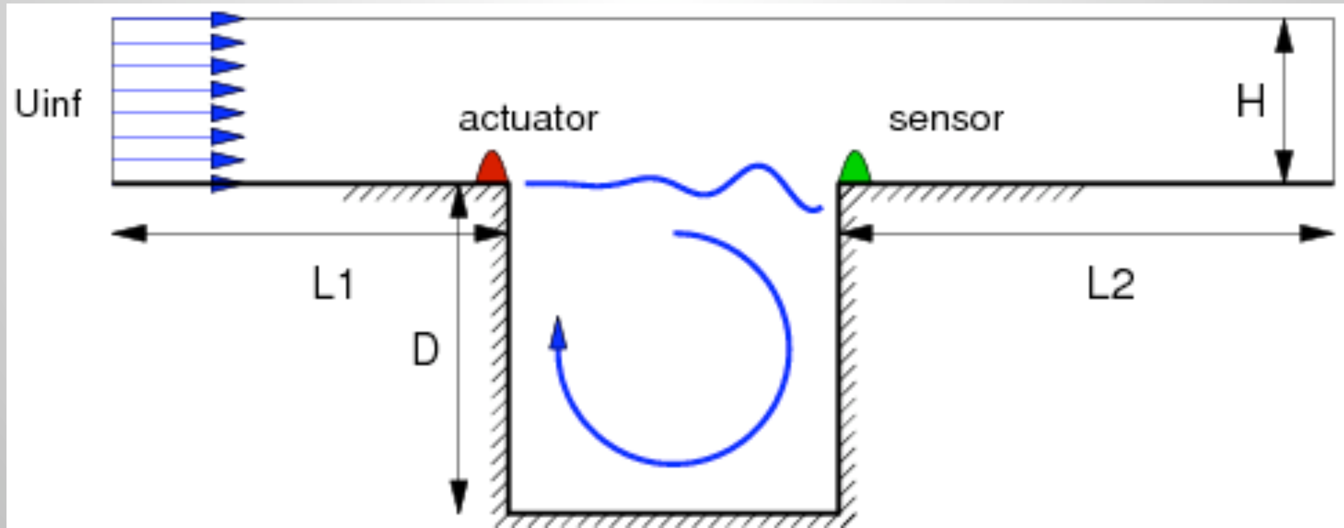

Generalizations

multiple inhomogeneous directions/complex geometry → global mode analysis

Examples of global modes: open cavity flow (two-dimensional)

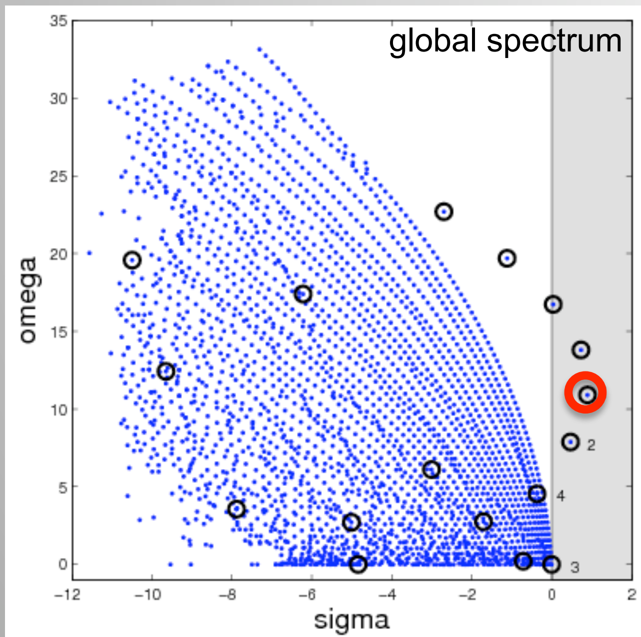

global mode

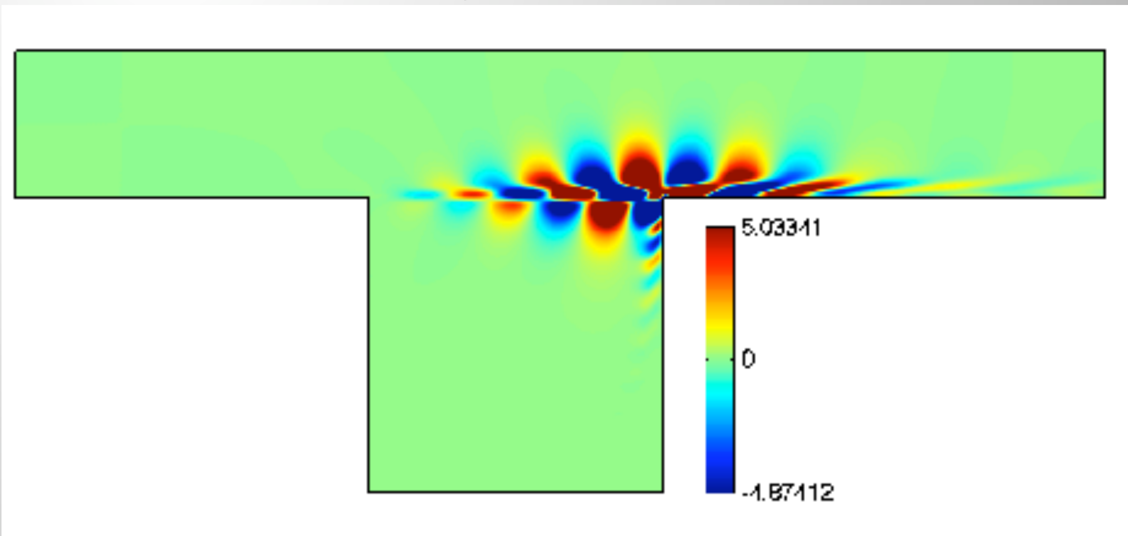

Generalizations

multiple inhomogeneous directions/complex geometry → global mode analysis

Examples of global modes: open cavity flow (two-dimensional)

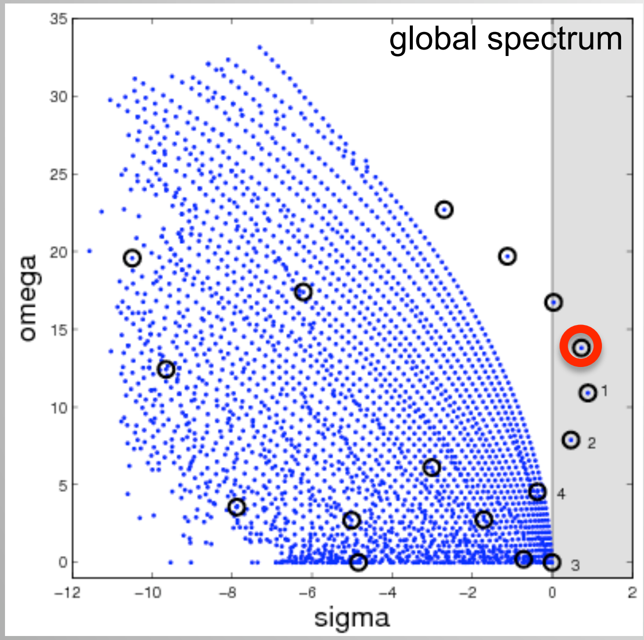

global mode

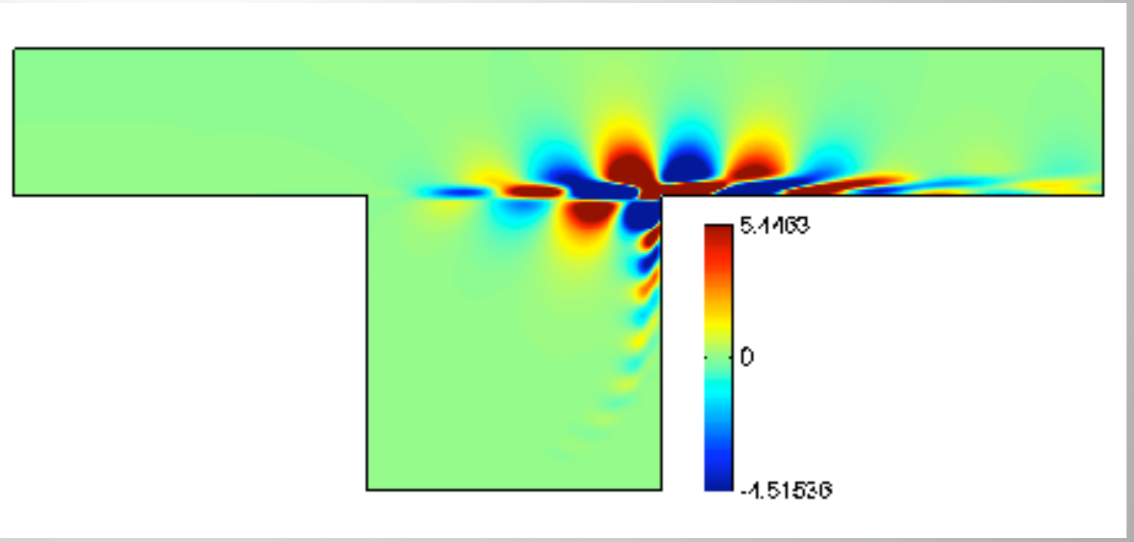

Generalizations

multiple inhomogeneous directions/complex geometry → global mode analysis

Examples of global modes: open cavity flow (two-dimensional)

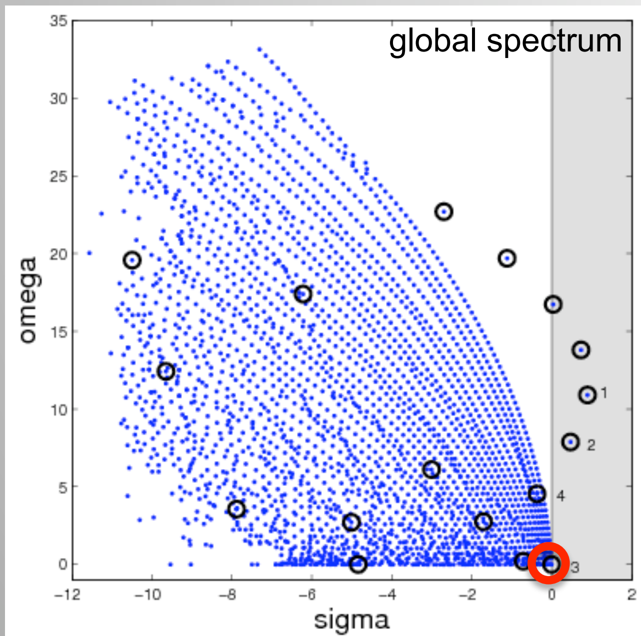

global mode

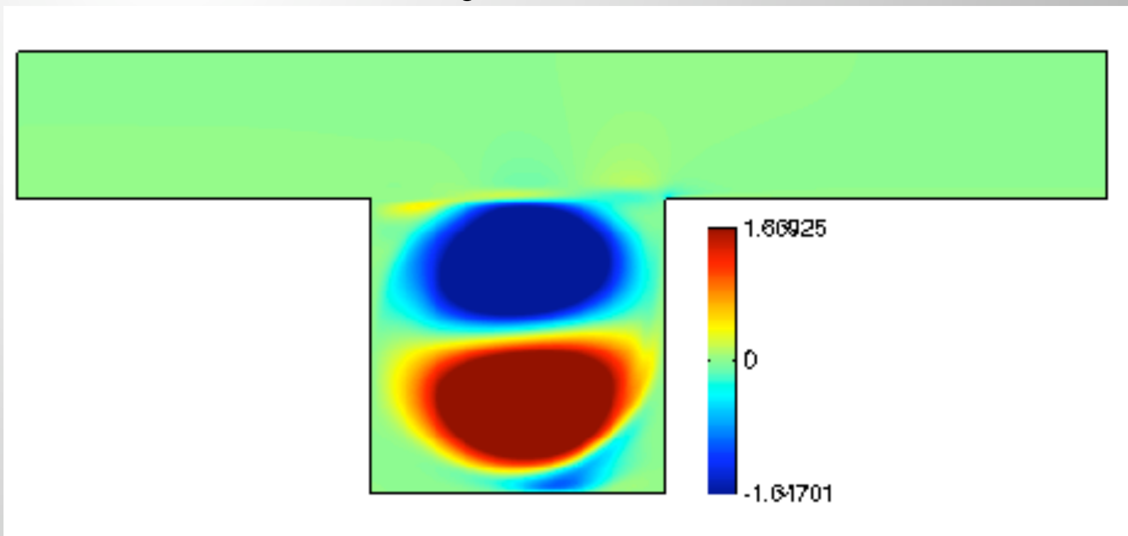

Generalizations

multiple inhomogeneous directions/complex geometry → global mode analysis

Examples of global modes: open cavity flow (two-dimensional)

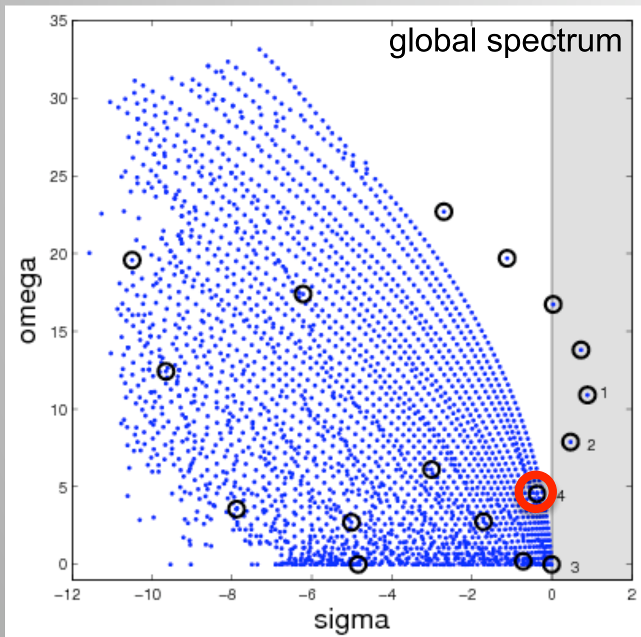

global mode

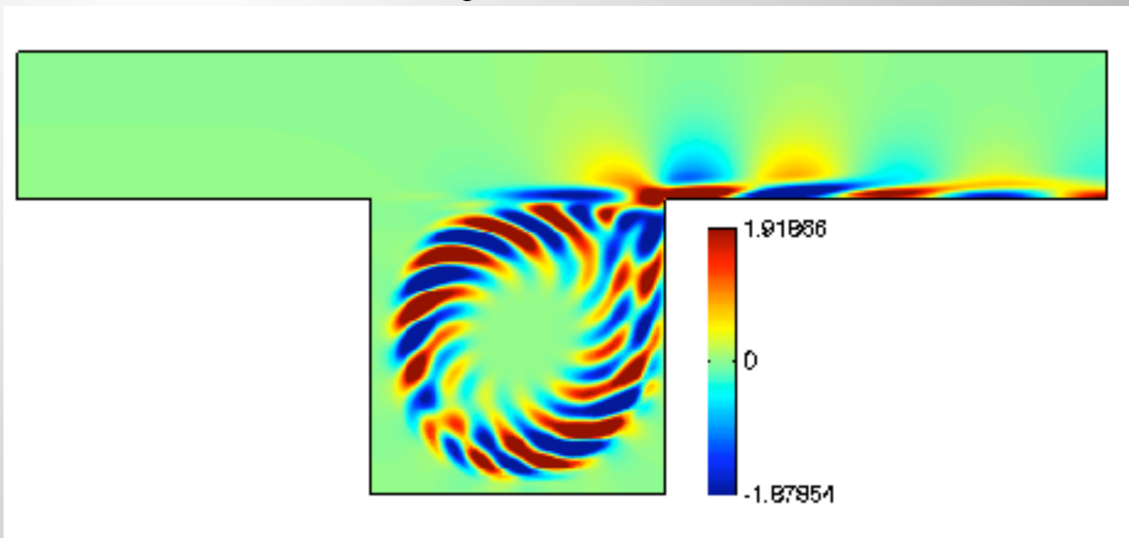

Generalizations

multiple inhomogeneous directions/complex geometry → global mode analysis

Examples of global modes: jet in cross flow (three-dimensional)

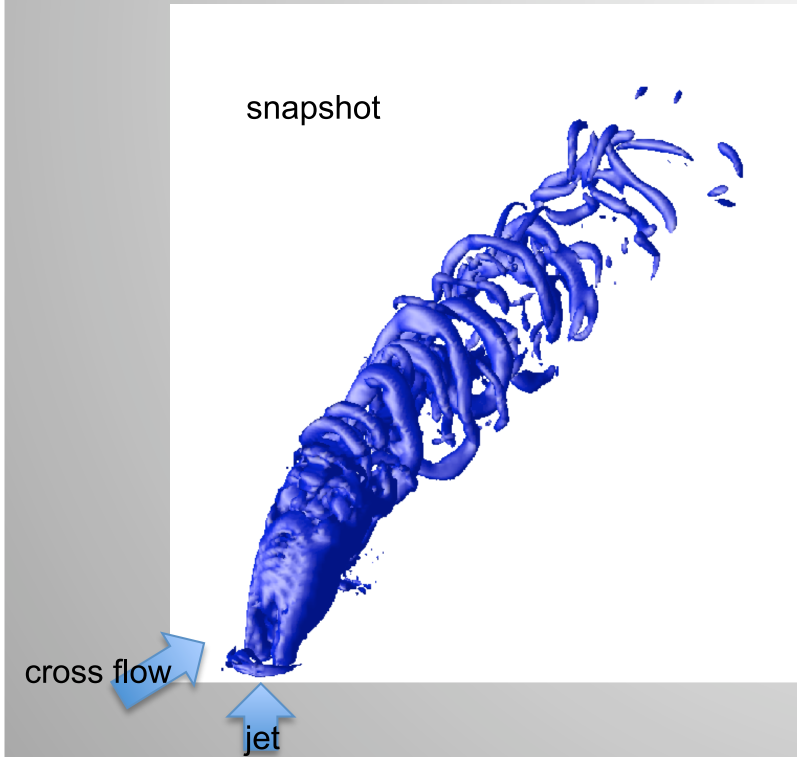

Arnoldi algorithm

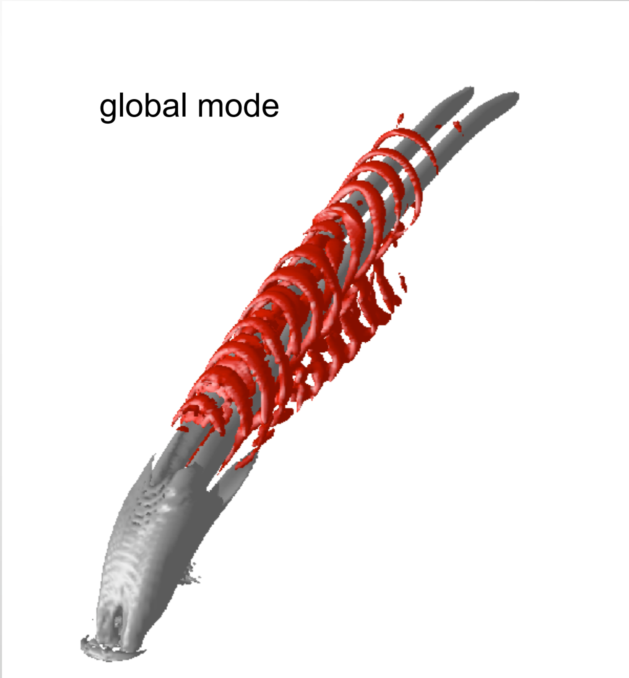

Arnoldi algorithm (a Krylov subspace technique) to compute the Hessenberg matrix H

```
q_k = A * q_{k-1};
for j=1 to k-1
    h_{j,k-1} = (q_j,q_k);
    q_k = q_k - h_{j,k-1}*q_j;
end
h_{k,k-1} = norm(q_k);
q_k = q_k/h_{k,k-1};
```

ARPACK

Jacobian-free framework

$$\mathrm{Aq}_k \approx \frac{\boxed{\mathcal{F}(\mathrm{Q}_0 + \varepsilon \mathrm{q}_k)} - \mathcal{F}(\mathrm{Q}_0)}{\varepsilon}$$

DNS

$$\mathrm{Aq}_k \approx \mathrm{Imag}\{\boxed{\mathcal{F}(\mathrm{Q}_0 + i\mathrm{q}_k)}\}$$

Summary

- Nonnormal operators are ubiquitous in fluid dynamics and thermo-acoustics.
- In many cases multimodal effects are more relevant than single-mode phenomena.
- Nonnormal analysis is computationally more involved; extensions to non-generic cases (time-dependent, nonlinear, stochastic, multi-dimensional) are possible.
- Nonmodal analysis gives a more accurate picture of fluid flow behavior.